February 2019
Ph.D. Dissertation

A large-scale neuroimaging study on brain morphometry in normal aging and prediction of Alzheimer's disease

Graduate School of Chosun University

Department of Life Sciences

Balaji Kannappan

A large-scale neuroimaging study on brain morphometry in normal aging and prediction of Alzheimer's disease

대규모 뇌영상 분석을 통한 노화과정의 뇌구조 변화 및
알츠하이머병 예측 모델 연구

February 2019

Graduate School of Chosun University

Department of Life Sciences

Balaji Kannappan

A large-scale neuroimaging study on brain morphometry in normal aging and prediction of Alzheimer's disease

Advisor: Prof. Kun Ho Lee

This dissertation is submitted to the Graduate School of Chosun University in partial fulfillment of the requirements for the degree of Doctor of Philosophy in Science

October 2018

Graduate School of Chosun University

Department of Life Sciences

Balaji Kannappan

This is to certify that the Ph.D. dissertation of Balaji Kannappan has successfully met the dissertation requirements of Chosun University

Chairman Chosun Univ. Prof. Jung Sup Lee _____

Member Chosun Univ. Prof. Kun Ho Lee _____

Member Chonnam Univ. Prof. Byeong C. Kim _____

Member Chosun Univ. Prof. Ho Yub Jung _____

Member Chosun Univ. Prof. Jungsoo Gim _____

December 2018

Graduate School of Chosun University

CONTENTS

LIST OF TABLES

LIST OF FIGURES

ABSTRACT

A large-scale neuroimaging study on brain morphometry in normal aging and prediction of Alzheimer's disease

Balaji Kannappan
Advisor: Prof. Kun Ho Lee, Ph.D.
Department of Life sciences
Graduate School of Chosun University

Aging is associated with structural changes in the brain, even in the absence of dementia or other pathological conditions. Hence, it is vital to understand the underlying physiological mechanisms of pathological and non-pathological aging. Regional morphology at micro anatomical scale is closely related to functional specialization. We analyzed the cortical and subcortical metrics such as cortical thickness (CT), surface area (SA) and volume changes in 1252 cognitively normal subjects using high resolution 3Tesla MRI data. The analysis showed cortical thinning and surface area reductions are initiating around the temporal regions. Especially, annual percentile changes of these neuro-morphometries showed alterations around the hippocampal region. Hippocampus is differentially vulnerable to normal and pathological aging and hence investigating the changes in the sub-regions would shed some light on the underlying pathophysiology. Based on

these results, we investigated the changes in the hippocampal subfield volumes classifying subjects based on the amyloid imaging, cognitive testing and other clinical diagnosis. The data showed specific changes in diagnostic groups. With all the neuro-morphometric data, we constructed a statistical prediction model for the classification of Alzheimer's disease and cognitively normal subjects. The complete study examines the East Asian specific structural changes during healthy cognitive aging and produces a capable prediction model for the diagnosis of Alzheimer's disease.

요약

대규모 뇌영상 분석을 통한 정상 노화 과정의 뇌구조 변화 및 알츠하이머병 예측 모델 연구

칸나빤 바라지

지도교수: 이건호, Ph.D.

생명과학과

조선대학교 대학원

뇌는 치매를 비롯한 퇴행성 뇌질환에 의해 구조적 변화가 일어나며 또한 병리학적 이상이 없는 정상적 노화 과정에서도 뇌위축이 일어난다. 따라서 질환에 의한 뇌구조적 변화와 정상 노화 과정에서 뇌구조적 변화의 차이를 이해하는 것이 무엇보다 중요하다. 뇌구조적 변화는 영역별로 차이가 있으며 특히 알츠하이머병의 경우 기능적으로 분화된 해마 세부 영역에서 미세한 차이를 규명하는 것이 중요하다.

본 연구에서는 고해상도 3-Tesla MRI뇌영상을 이용하여 1,252명의 인지적 정상 및 AD 전주기 환자들에 대한 피질 및 피질하 영역에 대한 피질 두께, 면적, 부피 등의 변화를 측정하였다. 특히 최신 FreeSurfer 방법을 적용하여 해마 세부 영역 부피를 측정하였다. 아밀로이드 영상에 기반하여 정상, 무증상, 전조증상, 알츠하이머성 치매의 단계로 병의 진행에 따라 피험자를 정밀진단 분류하였다.

노화 과정에서 측두엽의 피질 두께 및 면적 감소를 확인하였으며, 특히 해마 부피의 뚜렷한 위축을 확인하였다. 해마는 정상적 노화와 병리학적 노화에서 그 취약성이 다르게 나타나기 때문에 미세 해부학적 차이를 통한 근본적 메커니즘 규명이 무엇보다 중요하다. 따라서 해마 세부 영역 부피 분석을

통해, 병의 증세에 따라 대부분의 해마세부영역에서 단계적으로 위축되었으나, 특이적으로 Parasubiculum 영역에서는 전조증상 단계까지 위축이 지연됨을 확인하였다.

본 연구에서 아밀로이드 영상촬영, 인지 검사, 임상 진단 결과를 기반으로 분류된 피험자들의 해마 세부 영역 부피 변화를 분석하였으며, 진단 그룹별 유의미한 변화를 관찰하였다. 뿐만 아니라, 본 형태학적 측정 연구 결과를 바탕으로 인지적 정상 피험자와 알츠하이머성 치매 환자들을 분류할 수 있는 통계적 예측 모델을 개발하였다.

본 연구는 정상노화 과정에서 동아시안 특이 뇌구조적 변화를 설명했으며, AD 진행과정에서 미세 해마 구조의 변화를 규명하였고, 알츠하이머병을 진단 분류할 수 있는 뇌구조 기반 예측 모델을 개발하였다.

INTRODUCTION

Aging

Global population aged 60 or over is growing rapidly than any other age groups at a rate of about 3% per year. Approximately, 13% of the world population is at least 60 years old which is expected to rise to about 22% by 2050. Population of 80 or over is projected to triple by 2050 and expected to increase 7 times its value in 2017. In 2030, aged population are expected to outnumber children under age 10 and projections indicate that by 2050, 60 or over aged population will be more than youth and adolescents at ages 10-24 ((UN), 2017, Newgard and Sharpless, 2013). Particularly, Republic of Korea was defined by the United Nations as aged society in 2017. Within just 17 years after the country reached the point officially described as aging in 2000. It is also predicted that the country would become a super-aged society in 2026 ((UN), Korea, 2017).

The lifespan of every species is determined by the evolution and is influenced by many diverse factors, including biological mechanisms. Understanding the underlying structural, functional and systematic processes in greater detail and implementing appropriate interventions to promote healthy lifespan is of great importance. Aging is an integral part of the lifespan that is often simplistically understood as the continuing loss in

physiological integrity and subsequent impairment in functioning, ultimately leading to death (Kanasi et al., 2016). The process of normal aging was further bifurcated into usual and successful aging while acknowledging and differentiating pathological changes from those attributable to chronological aging (Rowe and Kahn, 1987). Two contrasting theories – the active theory and disengagement theory proposed in early 1960s introduced a distinct approach of successful aging. That is, "adding life to years" as opposed to "years to life" (Havighurst, 1961) which was later updated in the late 1990s (Rowe and Kahn, 1997) emphasizing that "growing older need not be synonymous with loss and decline". The theories and concepts of aging can be investigated through multi-directional studies focusing on aspects such as biological, biomedical, psychological and many others. The research community is divided on the exact definition and standards that define successful aging.

The successful aging could be described superficially with three components - active engagement with life, high cognitive and physical functional capacity and low probability of disease and disease related disability. Several age-associated changes in the human brain have been revealed from the anatomical, physiological and histological point of view. Previous report shows brain atrophy in normal aging as statistically inevitable with a gradual decline after the age of 60, with a yearly loss of 2-3

grams from a normal adult average weight, majorly attributable to the marked changes in the frontal lobe. Sulcal widening, progressive increase in ventricular volume, white matter changes related normal cognitive impairment and disruptions of white matter tracts consistent with cortical disconnection are all observed in the normal aging. Damage to the DNA, irreversible protein glycation, increases in glial cell activation and oxidative damage to proteins and lipids are certain changes that accompany the process of aging that maybe in part be the underlying reason for the age related increasing incidence of degenerative conditions such as Alzheimer's disease (Mrak et al., 1997, Terry et al., 1987).

There has been an unprecedented acceleration in the aging research over the recent years, particularly after the breakthrough finding about the rate of aging being controlled, at least in part, by genetic pathways and biochemical processes conserved in evolution. Studies have described nine tentative hallmarks that represent the common denominators of aging: epigenetic alterations, genomic instability, loss of proteostasis, telomere attrition, mitochondrial dysfunction, deregulated nutrient sensing, cellular senescence, stem cell exhaustion, and altered intercellular communication. The overall deterioration both physical and functional due to aging has been attributed as the primary risk factor for major pathologies in human, including diabetes, cardiovascular disorders, cancer and neurodegenerative

disorders (López-Otín et al., 2013). A complete understanding of the normal aging process would give us a standard for comparison against the abnormal or pathological aging.

Alzheimer's disease

Dementia is an umbrella term for a range of clinical syndromes characterized by continuing decline in two or more cognitive domains, including memory, personality and behavior, executive and visuospatial function, language, which interferes with the basic activities of daily life and loss of abilities to perform instrumental tasks. There is an overwhelming impact on the quality and quantity of life of the individual with dementia, subsequently, weighing down on their caregivers, friends and family, and the wider society with immense emotional, physical and economic burden that gradually intensifies as the patient symptoms progress affecting the mobility, communication and self-care. The worldwide prevalence is estimated to be around 46.8 million people, with the numbers projected to almost double every 20 years, posing to be the biggest global public health challenge. The recent estimate of the global costs of dementia represents around 1.09% of global GDP, excluding the informal care costs. The distribution of the costs can be divided into three categories: direct medical cost accounting for roughly 20%, while direct social sector costs and informal care costs accounting for roughly 40% each, respectively. Among them different forms of dementias, the most common form affecting around 60-80% of the cases is the Alzheimer's disease – a progressive neurodegenerative disease which is disabling and irreversible, causing a large socioeconomic burden. Alois

Alzheimer, a German clinical psychiatrist and neuroanatomist, initially described the Alzheimer's disease in 1906 after the autopsy study of an old woman with severe dementia. Alzheimer's disease is pathologically characterized by the presence of extracellular amyloid deposits with and without neuritic elements, and by intraneuronal changes including neurofibrillary tangles. Increasing age is the greatest known risk factor for the Alzheimer's disease and Alzheimer's is not a normal part of aging. Though, age increases the risk, it is not a direct cause of Alzheimer's. Approximately, 200,000 Americans under 65 years of age have been reported to have early onset Alzheimer's disease. On average, individuals live four to eight years after the diagnosis, but depending on other factors sometimes can live as long as 20 years (Prince et al., 2017, Hippius and Neundörfer, 2003, Hebert et al., 2013).

The most common and early symptom of Alzheimer's is difficulty in forming new memory and remembering recently learned information as changes typically start in the region of the brain responsible for learning and memory. Though, most individuals eventually notice some slow thinking and random problems with remembering with increasing age. Serious memory loss, confusion and other major changes including disorientation, mood and behavior changes, event, time and place related deepened confusions,

baseless suspicions about friends, family and professional caregivers and difficulty in speaking, swallowing and walking are certain characteristics of Alzheimer's disease.

Despite, the delayed clinical symptoms, microscopic changes in certain regions of the brain begins long before the first signs of memory loss. The human brain contains over 100 billion neurons or nerve cells making over a trillion connections. Each groups of neurons and connections work in an organized fashion to perform certain specified action. Alzheimer's disease interrupts and prevents the functioning of parts of these nerve cells and connections disrupting the regular functioning of the affected region, damaging and influencing the network of connections. Damage to these nerve cells and connections gradually causes an irreversible change to the brain. The two hallmarks of Alzheimer's disease are the beta-amyloid plaques that are abnormal deposits of protein fragments that build up in the spaces between the neurons and neurofibrillary tangles which are twisted fibers of another protein that build up inside the nerve cells. Certain studies have shown such changes associated with normal aging processes. However, the pattern and severity are far more in Alzheimer's disease (2018, Organization, May 2017).

The National Institute of Neurological and Communicative Disorders and Stroke and the Alzheimer's Disease and Related Disorders Association (NINCDS-ADRDA) proposed guidelines in 1984 for the clinical diagnosis of the Alzheimer's disease (McKhann et al., 1984) which was later revised in 2011 by the National Institute on Aging and the Alzheimer's Association (NIA-AA) charged workgroup (McKhann et al., 2011). Persistent memory complaints, hippocampal volumetric loss, beta-amyloid deposition detected by imaging or bio-fluid based biomarkers are certain criteria used for the early clinical diagnosis of Alzheimer's disease. Despite numerous studies, the findings that are identified are currently too inconsistent to reach firm and generalizable conclusions regarding underlying trends. Currently, there is no cure or preventive medication to stop or slow the disease.

Neuroimaging

Neuroimaging or a brain imaging is any imaging experimental technique that allows human or animal brain structure or function to be studied by ideally producing accurate spatial localization (for both structural and functional imaging) and timing (functional imaging) of cerebral structure, function and other related changes in the properties of the brain. The technique should be minimally invasive and capable of being performed multiple times to facilitate its use in development of therapeutic strategies and treatment monitoring. Multiple techniques have been used and certain most common and widely used methods are electroencephalography (EEG), positron emission tomography (PET), structural magnetic resonance imaging (MRI), functional magnetic resonance imaging (fMRI) and diffusion tensor imaging (DTI), each serving individual purposes. EEG has been used for the longest time. Following which PET has been available for the second longest period (in the order of around 40 years), and fMRI is the newest widely used technique. The EEG makes the closest approach to measuring neuronal activity directly but with considerably poor spatial mapping properties. The fMRI has emerged as the most widely used techniques recently for its functional brain mapping method as the location of the cerebral activity and alterations in the activity associated with the changes in the state of the brain either illness-determined or experimental seems to have been recent priority

in most recent researches. Among various techniques that are being used, the PET imaging is arguably the most invasive (as it involves administration of radioisotope).

Magnetic resonance imaging

Magnetic Resonance Imaging (MRI) is a medical imaging technique that is used to observe specific types of tissues non-invasively. The first MRI imaging was successfully acquired by Damadian in 1976. Magnetic resonance is also used in the Magnetic Resonance Spectroscopy (MRS) which was introduced as a chemical analytic method in order to identify molecules by their biophysical properties. The procedure provided an opportunity to study small metabolites with concentrations around 0.5-10mM, in vivo. Predominantly, the MRS is used in the fields of neurology, oncology and traumatology as the technique is highly sensitive to the soft tissue parts of the body (van der Graaf, 2010).

Structural MRI (sMRI) has been the widely used common tool for the investigation of trauma and other disease related changes in the brain for some considerable time. With the advent of the MRI technology for the use in the fields of psychiatry and neurology, the primary aim among the various focus area were to establish the neural correlates of various disorders. That is, to determine the region and degree of changes in the structure and function of the brain in comparison with other subjects from a suitable reference population. Identification of such regions in the subjects and further consecutively in a population of interest would result in the identification of objective quantifiable alterations in the function of the brain

or what could possibly a biological marker or biomarker of the particular disorder in question for the specified population. Further, these biomarkers can be used to test the effects of a drug treatment or rather be used in the therapeutic interventions (quantitative measures of the effectiveness of a drug or treatment or a therapy in restoring the normality).

The hardware required for the magnetic resonance has a large magnetic bore that produces static magnetic field B_0, time-varying magnetic field B_1 produced by a radio frequent RF-coil and gradient coils that allow for the selection of any region or volume of interest (ROI or VOI). In the recent decades, with the introduction of superconductive coils and the use of cryogenic coolants like liquefied helium, magnetic fields with varying strengths such as 1.5Tesla, 3Tesla, 7Tesla and up to 11Tesla have been produced and tested. Though, these have brought remarkable improvements in the resolution of the imaging, the cost for each have been on a steady rise. Constant improvements in the coil design to improve the sensitivity of the magnetic resonance systems and others have been made. sMRI provides good spatial resolution, is noninvasive and meets possible standards for structural analysis of the brain.

The sMRI produces multiple contrasts of the tissues of the brain like the T1 weighted, T2 weighted and others, with T1 being the largely used. The contrasts basically reflects how the magnetic resonance signals changes

over time in accordance to an exponential relaxation curve that describes how the magnetized spinning proton returns to its equilibrium state and realigns with the main magnetic field, after excitement by a radiofrequency pulse that is turned on and off. The energy that is generated when the protons return to the location determined by the external magnetic field of the scanner is detected via the head coil of the scanner. T1 weighted images which contrast solid and fluid properties as well as white versus gray matter are used for morphometric analyses of neuroanatomical brain volumes. Differences in contrast are caused by differential density of protons (Hornak, 2018)

CHAPTER 1

Cortical thickness has higher variance in healthy cognitive aging than other morphometric measurements

Abstract

We observed the structural changes in the brain associated with the process of cognitively healthy aging. Distinct influences that are contributing to the variations are examined through morphometries such as cortical thickness, cortical surface area, cortical gyrification and cortical and subcortical regional volumes. With over a thousand samples obtained using a single scanner and imaging procedures, we reviewed the changes of the cerebral cortex and subcortical regions. Brain undergoes structural changes which consecutively lead to functional changes even in the absence of neurodegenerative disease. Knowledge about the variations in the brain morphometries with respect to age and the distinct differences within each gender will help us understand if the atrophy rates are linear throughout the elderly life. The accumulations of this consistent gradual atrophy are misconceived when detected in the later stages or if there is accelerated atrophy especially in the later stages with every increasing year. Supposition changes across a wide range of 65-85 years were studied and the influences of the age and gender on the rate of changes on brain morphometries were

examined. The r-squared values of the total cortical volume could explain about 3.2%, total surface area could explain 1.5% and total cortical thickness could explain about 8.8% of the total variation in the brain morphology associated to increasing age. Thus, the comparative results suggest that the healthy cognitive aging process influences cortical thickness more than the other morphometries.

Keywords: Healthy cognitive aging, Cortical Volume, Cortical thickness, cortical surface area

1.1. Introduction

The area of brain aging research is yet to answer multiple core questions like which brain regions undergo change and which regions remain spared and why, the borderline between the non-pathological and pathological aging, the rate of atrophy and many others? One of the most intriguing questions among those is the concept of normal aging? Whether the process involves inevitable gradual structural and functional changes in the brain or if they remain unimpaired? In neurodegeneration and other aging abnormality related studies, cognitively intact subjects with similar age are presumably considered as controls. Though, the process of aging itself is shown to be associated with specific patterns of structural brain changes even in the absence of pathological conditions like dementia (Raz et al., 1998, Allen et al., 2002, Allen et al., 2005). Aging is among the high risk factors of neurodegenerative disease such as Alzheimer's disease (AD) and certain studies have also been performed on whether the Alzheimer is just an exaggerated form of aging rather than a disease (Ohnishi et al., 2001). Subsequently, it would rather be difficult to understand any neurodegenerative diseases including Alzheimer without knowing why it principally affects older brains. It is necessary to have a standard that accounts for changes associated with non-pathological aging for comparisons (Fjell et al., 2014a). Clarifications on multiple such issues would be available

only with the detailed large scale study of the cognitively healthy individuals with same imaging procedures.

Multiple studies have been performed on the age associated changes in brain morphometries primarily bifurcating based on the regions showing changes. The first category shows vulnerability in the prefrontal cortical regions (Tisserand and Jolles, 2003, Abe et al., 2008, Allen et al., 2005) with functions such as speed of processing, response inhibition and interference suppression, working memory and cognitive control that depends on the integrity of prefrontal cortex showing age-related decline (West, 1996, Raz et al., 1998). The second category that has repeatedly been implicated in the process of healthy cognitive aging includes the medial temporal lobe and regions around the hippocampus (Bigler et al., 2002, Du et al., 2006, Fjell et al., 2009a). The atrophy in the medial temporal lobe has gained a greater attention as both non-pathological and pathological aging have been shown to be involved (Fox et al., 2001, Killiany et al., 2002). Though, the rate of medial temporal lobe atrophy in the pathological aging has been found to be approximately twice than the non-pathological aging (Jack et al., 1998). The role of the medial temporal lobe in episodic memory which has shown age-related decline (Verhaeghen et al., 1993) and studies predicting prospective memory decline in non-pathological aging has added to the greater attention (Rusinek et al., 2003, Rodrigue and Raz, 2004). Systematic characterization

of the rate and level of atrophy in the cognitively healthy aging is vital for therapeutic interventions targeting age-related disorders.

Voxel based morphometry has been customarily used in the volumetric studies of the brain (Ashburner and Friston, 2000, Good et al., 2001). However, there has been recent boost in the advent of new computational methods of surface based morphometry that provide more detailed and specific morphological measures such as cortical gyrification, cortical and sub-cortical volumes and its components cortical surface area, cortical thickness and others. Study approaches based on these surface based values have shown to be more sensitive than the voxel based analysis in better understanding the global and regional structural changes of the brain (Hutton et al., 2009). Cognitive healthy aging and AD show volumetric reductions while surface area reduction and cortical thickness reductions were exclusively associated with cognitive healthy aging and AD respectively (Dickerson et al., 2009b). Many variables including gender, educational level, intracranial volume in volumetric analyses, apoe genotyping, β-amyloid burden and interactions among these factors has been shown influencing the process of aging. The growing interest on comprehensively understanding the effects of aging both pathological and non-pathological would be relatively straightforward through the studies based on thickness and surface area than voxel based morphometry.

Most previous studies have considered the brain volumes or thickness or surface area or cortical gyrification separately in the studies. The purpose of the current study is to provide a comprehensive picture of all the cortical morphometries obtained through the large scale analyses. Though, the volumes obtained can be divided into its constituent parts – surface area and thickness. We expected to study the distinction between them as heterogeneity has been observed.

1.2. Methods

Study participants

The regional ethics committee approved the research study and written consent were obtained from the participants (or family members or care givers where appropriate). The data presented in the current study are based on T1-weighted structural magnetic resonance images of over 1000 samples assembled by the National Research Center for Dementia (NRCD) at Chosun University in Gwangju, Republic of Korea. A battery of neuropsychological tests that assess language, attention, memory, visuospatial and executive function was administered to all participants. Control samples did not show any evidence of neurological disease or impairment in cognitive function or activities of daily living. Subjects with history of head trauma, focal lesion on brain MRI and medical or psychiatric causes that could affect cognitive decline were excluded.

MRI Acquisition

Contiguous 0.8 mm sagittal MPRAGE images of the whole brain examined at NRCD were acquired using 3T MR scanner (Skyra, Siemens) with the following parameters: TR = 2300 ms; TE = 2.143 ms; TI = 900 ms; 9 flip angle; FoV = 256x256; matrix = 320x320; number of slices = 178.

MRI preprocessing

High resolution structural T1-weighted images were processed using the FreeSurfer software package (Athinoula A. Martinos Center for Biomedical Imaging, Harvard University, Cambridge, MA, USA) (v5.3.0) on a Linux environment using a 64-bit CentOS 7 operating system. The exclusive documentation of the freesurfer pipeline and methodologies can be found elsewhere (Dale et al., 1999, Fischl et al., 1999, Fischl et al., 2002, Fischl et al., 2004a, Fischl et al., 2004b). A complete automated processing including cortical and subcortical labelling using the Desikan-Killiany atlas was performed on each subject. The freesurfer processing stream involves performing motion correction, NU(non-uniform intensity normalization) for intensity inhomogeneity correction, image registration using affine transformation (6, 9 or 12 degrees of freedom) to Talairach space (J. Talairach, 1988) , and skull-stripping based on combination of watershed algorithm and deformable template model (Ségonne et al., 2004) or the removal of non-brain tissues. Then, the image volume is intensity normalized

following non-linear warping of the atlas brain image to subject brain image which in turn is utilized in atlas-based tissue segmentation, in labeling the subcortical structures, brain stem, cerebellum, and cerebral cortex. The next step in FreeSurfer is to generate topologically correct cortical surface representation per hemisphere. Cortical surface lies either at the WM/GM tissue interface or at the GM/CSF tissue interface. Each hemisphere's cortical surface representation is mapped automatically to a standard spherical coordinate system. Key components of the surface mapping include surface inflation with minimal metric distortion, projection to spherical coordinates, topology correction, and surface based warping to align anatomically homologous points. Mapping to the standard spherical coordinate system defined by FreeSurfer atlas brain allows for automated anatomical parcellation of cortex into gyral regions. Surface parcellation is then extended to GM volume, yielding parcellation of GM tissue sheet and regional cortical volumes. The entire computation took about 16-24 hours.

Imaging analyses

To assess the effect of age with changes in the brain morphometries, we used a general linear model (GLM) with age as the main factor and gender, level of education and total intra cranial volume (ICV) as covariates (when applicable). All the possible values were separately evaluated with separate GLM. The random field theory (RFT) based method was used for

correction of multiple vertex wise comparisons, and cortical clusters with a family wise error (FWE) corrected $p < 0.05$ (uncorrected $p < 0.001$) were considered significant. All the GLM analyses were implemented using Surfstat (Worsley et al., 2009).

Statistical analyses

All statistical analysis was performed using IBM SPSS Statistics (Version 23.0. Armonk, NY: IBM Corp.). To begin with, the total cortical volume, total surface area and average total cortical thickness of the whole brain were derived by combining the left and right hemisphere values. Separate analyses were performed with the age as the independent variable, and each morphometric variables as the dependent variable. Analyses were performed separately for each hemispheres as evidences of asymmetries in the age associated brain changes are shown (Raz et al., 1997). Gender, intracranial volume and level of education were corrected to avoid any confounding effects when applicable. The type I error used for statistical significance was $\alpha \leq 0.05$ for all analyses. The relationship between any two variables was calculated using Pearson correlations.

Thickness measures at surface locations from the following 34 pairs of bilateral FreeSurfer cortical regions (68 ROIs in total) were analyzed in this study

ID	ROI name
1	Banks of the superior temporal sulcus
2	Caudal anterior cingulate
3	Caudal middle frontal gyri
4	Corpus collosum
5	Cuneus
6	Entorhinal cortex
7	Fusiform gyri
8	Inferior parietal gyri
9	Inferior temporal gyri
10	Isthmus cingulate
11	Lateral occipital gyri
12	Lateral orbitofrontal gyri
13	Lingual gyri
14	Medial orbitofrontal
15	Middle temporal gyri
16	Parahippocampal gyri
17	Paracentral lobule
18	Pars opercularis
19	Pars orbitalis
20	Pars triangularis
21	Pericalcarine gyri
22	Postcentral gyri
23	Posterior cingulate
24	Precentral gyri
25	Precuneus

ID	ROI name
26	Rostral anterior cingulate
27	Rostral middle frontal gyri
28	Superior frontal gyri
29	Superior parietal gyri
30	Superior temporal gyri
31	Supramarginal gyri
32	Frontal pole
33	Temporal pole
34	Transverse temporal pole

Keywords: ROIs, regions of interest.

1.3. Results

The average total cortical volume of the cohort was 410.52±37.54 cm^3. Average total surface area and average total cortical thickness of the whole cortex were 1510.20±186.17 cm^2 and 4.73±0.10 mm respectively. Correlation analyses showed that the age was significantly negatively correlated ($r = -0.17, p < 0.001$) with total cortical volume, significantly negatively correlated ($r = -0.12, p < 0.001$) with total surface area and significantly negatively correlated ($r = -0.29, p < 0.001$) with total cortical thickness. Additionally, the total cortical volume could explain about 3.2%, total surface area could explain 1.5% and total cortical thickness could

explain about 8.8% of the total variation in the brain morphology associated to increasing age. These effects represented the global reductions of 1.33 cm^3 per year in the total cortical volume, 3.51 cm^2 per year in total surface area and 0.01 mm per year in global average cortical thickness.

The individual hemispheric results for each morphometries against age can be found in the table 1. Additionally, the vertex-wise analyses of the cortical surface area and the cortical thickness revealed significant variations in the temporooccipital lobe and parts of frontal region as summarized in figure 1 & 2.

Table 1. Individual hemispheric results for each morphometries

Metrics	Left					Right				
	r	*p*	*rsq*	*B*	*SE (df=1006)*	*r*	*p*	*rsq*	*B*	*SE (df=1006)*
Vol	-0.18	2.47E-09	0.03	-680.74	115.36	-0.1744	1.24E-8	0.03	-655.71	116.71
SA	-0.12	3.30E-5	0.01	-177.15	44.22	-0.1223	4.90E-5	0.01	-173.90	44.46
thk	-0.29	5.42E-22	0.08	-5.10E-3	5.23E-4	-0.2885	4.37E-21	0.08	-5.04E-3	5.28E-4

Vol; Volume, SA; Surface area, thk; Thickness.

p-value < *0.05* was considered as statistically significant.

1.4. Discussion

The current study examined the age associated structural changes on distinct brain morphometries that could be obtained from automated surface reconstruction (Dale et al., 1999, Fischl et al., 1999, Fischl et al., 2002, Fischl et al., 2004a, Fischl et al., 2004b). Earlier, the structural changes in the brain related to aging effects were studied extensively using the voxel based methods (Good et al., 2001, Grieve et al., 2005, Kalpouzos et al., 2009) or using region-of-interest based volumetric analyses (Raz et al., 1997, Jernigan et al., 2001). With the advent of suitable automated methods that provide diversified metrics for the analyses of total and regional values such as cortical surface area, cortical thickness and sulcal characteristics in addition to the previous calculations of cortical volume. The analyses of the effects of aging on the brain morphology using these numerous metrics have interested many. Yet, the use of all the supplied metrics for detailed analyses remains scarce. In the present study, three measured morphometric components were studied and showed age associated analogous reductions that were not uniform. The nature of the morphometric differences varied. Though there were convergent patterns of variations, notable disparities were also clearly observed between the morphometries.

Firstly, the region of the brain that showed common differences in the global total metric reductions. Of all the brain regions, the temporal region

showed clear reduction in morphometric values. When compared to the global trend, the temporal cortex showed a significantly accelerated decrease in cortical surface area and cortical thickness with age (as illustrated in figure 6 & 3 respectively). Our results are in line with several other studies that show reductions in temporal regions and regions around hippocampus (Fox et al., 2001, Bigler et al., 2002, Du et al., 2006). The hippocampal atrophy as obtained from the structural magnetic resonance imaging analysis has been a well-established structural imaging biomarker in the guidelines of diagnostic criteria for the early diagnosis of Alzheimer's disease (Jack et al., 2018). The hippocampus plays a key role in the memory functions. Disruption in the memory especially episodic memory is among the earliest signs of non-clinical symptoms that are characteristics of the Alzheimer's disease. Interestingly, the hippocampus and the medial temporal lobe have been repeated implicated in the process of healthy cognitive aging. Thus, adding to the heightened interest in studying further about these regions in detail (Bigler et al., 2002, Du et al., 2006, Fox et al., 2001, Killiany et al., 2002).

The cortical thickness values (around 8.8%) showed significant variations than the surface area (around 1.5%) or the volume (around 3.2%) in explaining the age related structural changes. Based on this, we might propose that cortical thickness and then the cortical volume are quantitatively more informative for age associated structural morphometric changes across

the brain. In the field of imaging genetics, the structural neuroimaging phenotypes are used in the gene identification for possible genetic variation. The procedure providing only the cortical volume measurements have been reported to be less sensitive than those that involves the measurement of differences in the cortical thickness values (Winkler et al., 2010). One possible explanation could be that the underlying mechanisms of the age associated structural changes affect more specifically the cortical thickness than the volume which rather is a synergistic measure that integrated the cortical thickness and the folding. Certain studies suggest that chronic and low-grade inflammation with the increasing age may be characterized by concomitant cortical thickness increase and surface area decrease (Cevenini et al., 2010, Solana et al., 2012).

Studies on structural changes in the brain with respect to age may show variability in their findings that may be in part, due to the differences in the study samples and other clinical variables and demographics such as level of education, genetic variations, vascular risk and amyloid beta (Gonzalez et al., 2015, Villeneuve et al., 2014, Luders et al., 2006b). In particular, the sexual dimorphism in the differential trajectories of age related structural changes have been shown (Murphy et al., 1996, Coffey et al., 1998, van Velsen et al., 2013). Certain regions do show changes over time that might be captured only in the longitudinal studies but not in cross

sectional studies (Fjell et al., 2014b). Left-right hemispheric asymmetry and influence of gender on the degree of asymmetry have earlier been reported (Luders et al., 2006a). Thus, we performed the study on both the hemispheres separately to analyze for global hemispheric asymmetries. However, we did not observe any significant hemispheric differences in all the three morphometries. The discrepancy may be due to the difference in the study population or the ethnic differences between the study populations. In the current study, we observed for changes in the global metrics whereas earlier studies have analyzed region of interest based hemispheric asymmetries. Additionally, earlier studies performed with large cohorts of individuals over 60 years of age have included the primary cortices in their patterns of regions that were affected by age (Ziegler et al., 2010, Lemaitre et al., 2005, Salat et al., 2004) albeit a total replication of this in studies with smaller cohort of individuals over 60 years has not been observed (Fjell et al., 2009b, Sowell et al., 2003). Thus, we could suggest that the age related decline in the primary cortices occur in the later ages.

Cortical volume, cortical thickness and the cortical surface area – the three structural morphometric measures studies in the current study are inter-related and linked to each other on a simple mathematical equation, the volume is the product of surface area over the thickness. However, all three metrics may not be equally sensitive to the cortical atrophy related factors

such as aging or other age related disorders, and thus may represent their own specificity. Region of interest based study on healthy cognitive aging has shown preferential effect on the surface area while larger reduction of cortical thickness was seen in Alzheimer's disease. Similarly, based on the current study, we theorize that all the morphometries exert differential influences across the cortical regions to aging. Although, all the metrics seem to be interconnected, a detailed correlation is not well understood and warrants further investigation. In all possible ways, we can propose that these metrics combined could provide complementary information that may help in understanding the underlying mechanism of healthy cognitive aging.

Despite current study providing the descriptions on the age related structural changes in the brain morphometries with respect to healthy cognitive aging. The results observed in the current study are the age differences rather than age-wise changes which can explicitly be shown only through longitudinal studies. The obtained results may be biased due potential cohort based differences. The present study illustrated the general features of healthy cognitive aging. The patterns of global structural changes should be further investigated, as the information could provide vital implications for understanding sensitive effects of aging in cognitively normal individuals.

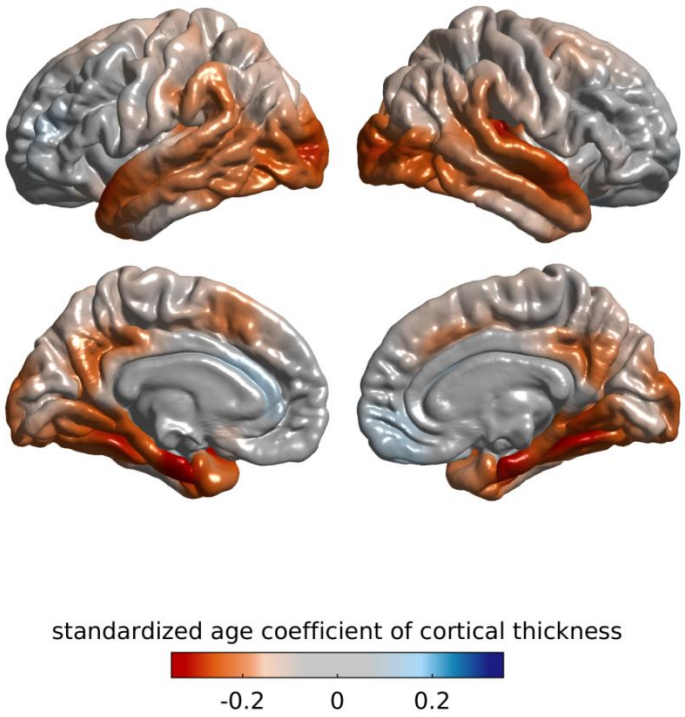

Figure 1. Cross-sectional estimates of cortical thinning around the hippocampus in healthy elderly (n = 1008). Adjusted for sex, years of education and estimated intracranial volume.

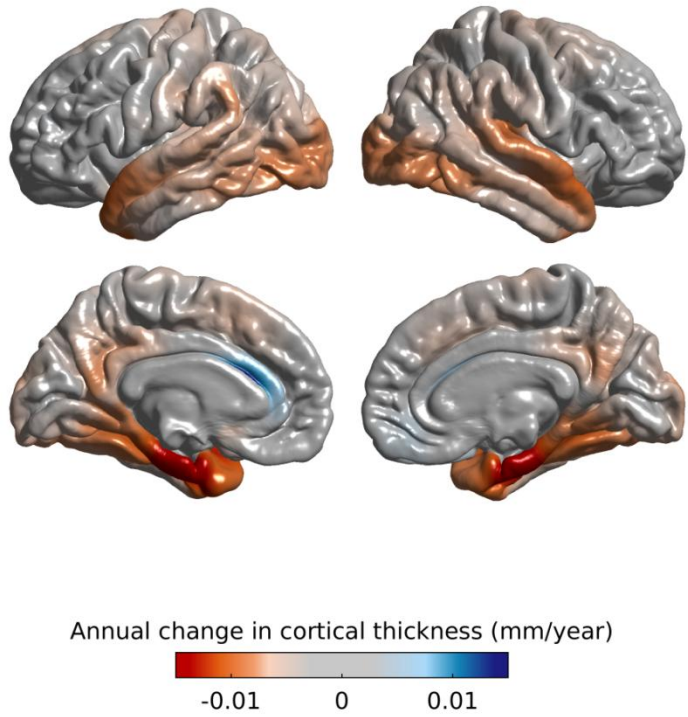

Figure 2. Annual change in cortical thickness (mm/year) estimated in healthy elderly (n=1008). Adjusted for sex, years of education and estimated intracranial volume.

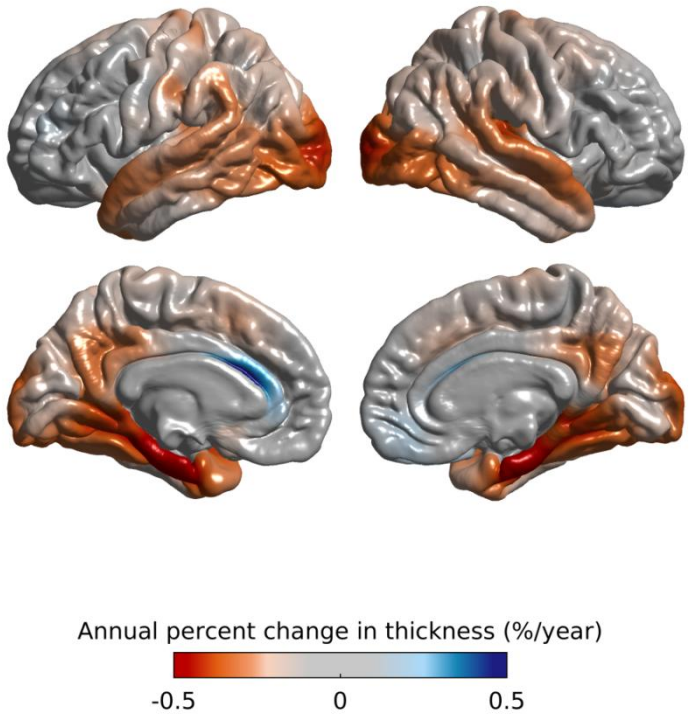

Figure 3. Percentile annual change in cortical thickness (% per year) estimated in healthy elderly (n=1008). Adjusted for sex, years of education and estimated intracranial volume.

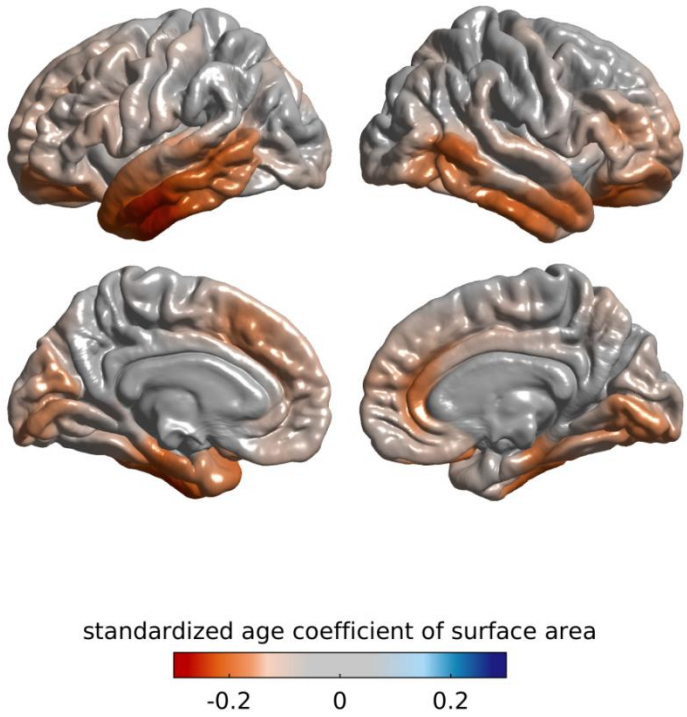

Figure 4. Cross-sectional estimates of cortical surface area reduction around the middle and inferior temporal regions in healthy elderly (n = 1008). Adjusted for sex, years of education and estimated intracranial volume.

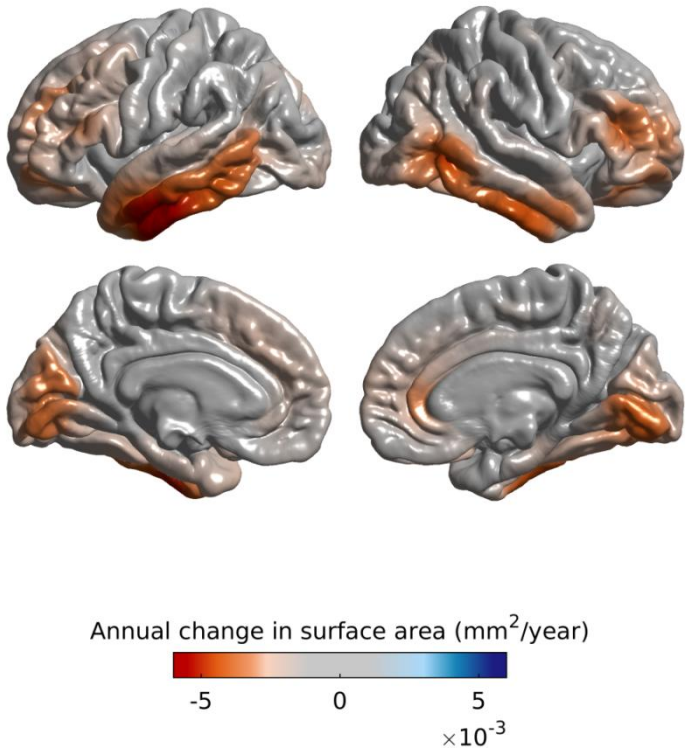

Figure 5. Annual change in cortical surface area (mm^2/year) estimated in healthy elderly (n=1008). Adjusted for sex, years of education and estimated intracranial volume.

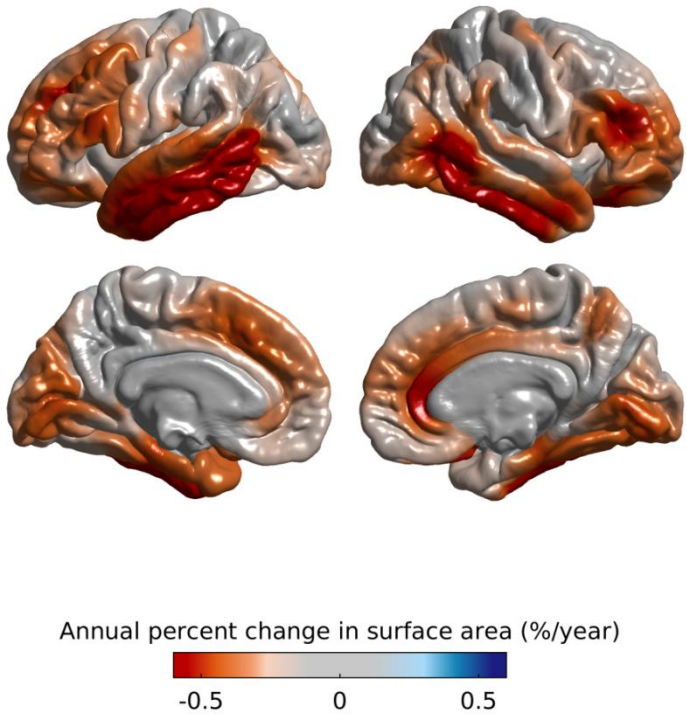

Figure 6. Percentile annual change in cortical surface area (% per year) estimated in healthy elderly (n=1008). Adjusted for sex, years of education and estimated intracranial volume.

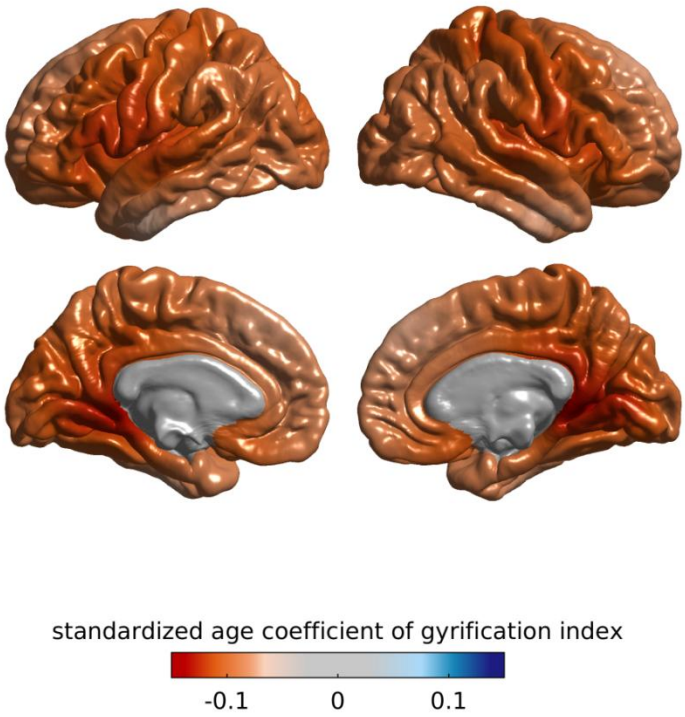

Figure 7. Cross-sectional estimates of cortical gyrification index reduction in healthy elderly (n = 1008). Adjusted for sex, years of education and estimated intracranial volume.

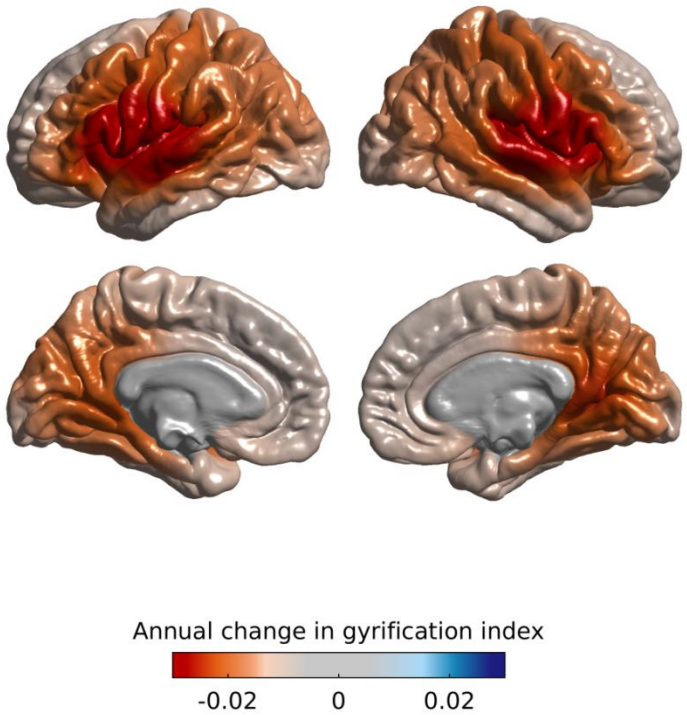

Figure 8. Annual change of cortical gyrification index estimated in healthy elderly (n=1008). Adjusted for sex, years of education and estimated intracranial volume.

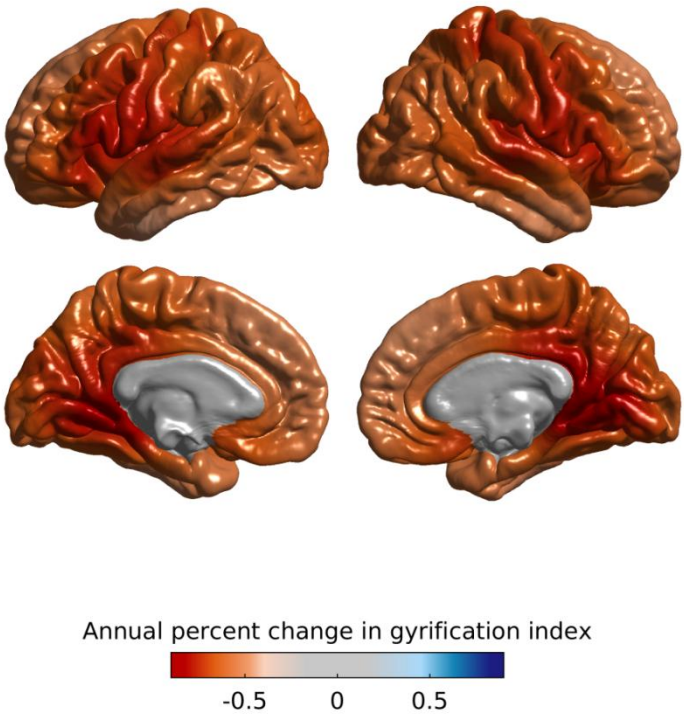

Figure 9. Percentile annual change in cortical gyrification index (% per year) estimated in healthy elderly (n=1008). Adjusted for sex, years of education and estimated intracranial volume.

CHAPTER 2

Hippocampal subfield volumetric analysis of asymptomatic, prodromal and Alzheimer's disease subjects

Abstract

Studies on changes in hippocampal subfield volume in association with the β-amyloid burden and cognitive status in Alzheimer's disease (AD) and stages preceding AD are limited. We checked for differences in hippocampal subfield volumes across 478 subjects with the intent to observe any variations, specific for subject groups: normal controls, asymptomatic AD, prodromal AD and cognitive impairment that are not dementia, classifying based on cognitive status and amyloid burden. Cognitively unimpaired β-amyloid positive and negative groups did not show significant volume differences. However, MCI β-amyloid positive and negative showed significant bilateral differences in hippocampal subfields: hippocampal tail, CA1 & 4, Molecular layer (ML), granule cells/molecular layer/dentate gyrus (GCMLDG) and right CA3. The findings suggest that the early deposition of the amyloid in the cognitive normal stages is not accompanied by significant bilateral neurodegeneration. However, subfield volume loss associated with the β-amyloid burden may be characterized by more symmetrical atrophy in CA regions than other hippocampal subfields.

Keywords: hippocampal subfield, amyloid imaging, structural MRI, cognitive status.

2.1. Introduction

Alzheimer's disease (AD) is characterized by the aggregation of abnormal amyloid-beta (Aβ) protein forming the neuritic or the β-amyloid plaques, neurodegeneration and neurofibrillary tangles of tau protein (Braak and Braak, 1991, Terry et al., 1991). Studies have used these hallmarks as AD associated biological markers (biomarkers) and these biomarkers do not reach abnormal levels simultaneously but do so consecutively. Subtle and detrimental accumulation of Aβ deposition is expected to initiate the continuum from normal cognitive status to MCI to AD dementia and it is believed to start at least two decades prior to the onset of any other clinical symptoms (Villemagne et al., 2013, Jack et al., 2009). β-amyloid imaging provides a critical adjunct to the diagnostic guidelines of asymptomatic stages of AD, when the disease modifying therapeutic intervention might be of the most beneficial (Sperling et al., 2011) and is expected to boost the overall confidence of the AD diagnosis and influence the clinical decisions (Schipke et al., 2012). Studies report that the diagnostic certainty and planned management in subjects have notably been amplified with the use of amyloid imaging thus may be useful in detecting preclinical AD state (Reiman et al., 2009, Mintun et al., 2006, Pike et al., 2007, Aizenstein et al., 2008).

Despite the advantages, study (Roberts et al., 2013) illustrates the ethical and practical issues associated with the amyloid imaging. For instance, legal safeguards, high cost not currently covered by Medicare or other insurances and unclear implications on family members makes it demanding for the widespread use (Newberg and Alavi, 2010, Roberts et al., 2013). Most importantly, approximately 10-30% of cognitively normal elderly test positive for amyloid imaging (Klunk et al., 2004, Mintun et al., 2006, Pike et al., 2007). The Amyloid Imaging Taskforce (AIT) convened by the Alzheimer's association and the Society of Nuclear Medicine and Molecular Imaging explains the appropriate use criteria for amyloid PET. It reports appropriate and inappropriate situations for the use of amyloid PET and states the use of amyloid PET in asymptomatic individuals and subjects with cognitive complaint that is unconfirmed on clinical examination as inappropriate (Johnson et al., 2013). Thus, use of amyloid imaging is restricted. The current situation thus warrants for a plausible approach which is comparatively commonplace technology and provides complimentary information, widely accepted and equally vital for the better selection of candidates for evaluation.

In the AD continuum, distantly following the Aβ deposition is the hippocampal volume atrophy approximately half a decade prior to other symptoms such as episodic memory, grey matter volume losses and

deterioration in the non-memory cognitive domains (Villemagne et al., 2013). It is supposed that the cognitive memory impairment associated with the disease progression might be caused by the β-amyloid induced hippocampal atrophy (Mormino et al., 2009). The quantitative estimates of automated structural MRI can serve as an *in vivo* surrogate for the severity of disease in various stages of disease progression (Desikan et al., 2009, Grundman et al., 2002, Fleisher et al., 2005, DeCarli et al., 2007). Hippocampal volumetry is among the highly discussed and studied quantitative magnetic resonance imaging (MRI) measure and considered a powerful non-invasive biomarker in diagnostic criteria and clinical trials for AD (Jack et al., 2011). With respect to the early AD detection, the hippocampal volumetric approach wins over the whole brain or the whole cortex approach, as it provides a straightforward and discernible index for use (Cuingnet et al., 2011). However, hippocampus is a non-homogeneous structure with histologically distinct subfields like subiculum and presubiculum, cornu ammonis (CA1-3), fimbria and dentate gyrus (DG). Each subfield believed to be functionally distinct, performing functions related to learning and memory, certain aspects of motor control, regulation of emotional behavior and regulation of hypothalamic functions among others (Duvernoy, 2005). Despite being long established, the limitations of the MRI resolution and lack of consistent and reliable segmentation methods

have traditionally forced the researchers to consider the hippocampus as a single homogeneous structure indifferent to the potential information that the sub regions could provide (Mormino et al., 2009, Fletcher et al., 2016, Jack et al., 2014). With the recent advances in the segmentation techniques, quick, reproducible and automatic segmentation of hippocampus into its various subfields is possible (Iglesias et al., 2015). The process of normal aging and the AD associated aging have varying effects on each subfields and also the adverse effects of various neuropsychological disorders are selective on the subfields and not diffuse on the whole hippocampus (West et al., 1994, Lucassen et al., 2006). β-amyloid pathophysiology catalyzes or increases the process of neurodegeneration but the rate of β-amyloid deposition is not influenced by the hippocampal neurodegeneration (Jack et al., 2014). Few studies (Storandt et al., 2009, Hedden et al., 2009) have reported significant hippocampal atrophy in β-amyloid positive cases whereas few others do not (Bourgeat et al., 2010, Dickerson et al., 2009a).

Here, we investigate the volumetric differences in the hippocampal subfields classifying the subjects based on their cognitive status and β-amyloid burden. In addition, we like to investigate the hemispheric asymmetry to understand lateralization of the hippocampal regions. We expect volumetric differences would characterize each group, which consecutively can be used to classify the subjects prior to the use of amyloid

imaging. Exploiting the synergistic information from both imaging biomarkers and the cognitive status associated with the pathophysiology of AD will offer new opportunities for the early prediction and we believe that the collective information acquired would be better than the information obtained using either in isolation.

2.2. Methods

Study participants

The regional ethics committee approved the research study and written consent were obtained from the participants (or family members or care givers where appropriate). Probable AD diagnosis was made based on National Institute of Neurological and Communicative Diseases and Stroke/Alzheimer's Disease and Related Disorders Association (NINCDS-ADRDA) Alzheimer's criteria (McKhann et al., 1984). As summarized in Table 1, Total of 478 study subjects (Normal controls (n=192; β-amyloid negative cognitively unimpaired[NC-]), Asymptomatic AD (n=34; β-amyloid positive cognitively unimpaired[Asymptomatic AD or NC+]), cognitive impairment that are not dementia (CIND) (n=118; β-amyloid negative mild cognitive impairment[MCI-]), prodromal AD (n=34; β-amyloid positive mild cognitive impairment[Prodromal AD or MCI+]), Alzheimer's disease dementia negative (n=30; β-amyloid negative severe cognitive impairment[non-AD dementia]) and Alzheimer's disease dementia

(n=70; β-amyloid positive severe cognitive impairment[ADD]) were assembled by the National Research Center for Dementia (NRCD) at Chosun University in Gwangju, Republic of Korea. A battery of neuropsychological tests that assess language, attention, memory, visuospatial and executive function was administered to all participants. Control samples did not show any evidence of neurological disease or impairment in cognitive function or activities of daily living. Subjects with history of head trauma, focal lesion on brain MRI and medical or psychiatric causes that could affect cognitive decline were excluded.

MRI Acquisition

Contiguous 0.8 mm sagittal MPRAGE images of the whole brain examined at NRCD were acquired using 3T MR scanner (Skyra, Siemens) with the following parameters: TR = 2300 ms; TE = 2.143 ms; TI = 900 ms; 9 flip angle; FoV = 256x256; matrix = 320x320; number of slices = 178.

MRI data processing

High resolution structural T1-weighted images were processed using the FreeSurfer software package (Athinoula A. Martinos Center for Biomedical Imaging, Harvard University, Cambridge, MA, USA) (v5.3.0 & v6.0.0) on a Linux environment using a 64-bit CentOS 7 operating system. The exclusive documentation of the freesurfer pipeline and methodologies can be found elsewhere (Dale et al., 1999, Fischl et al., 1999, Fischl et al.,

2002, Fischl et al., 2004a, Fischl et al., 2004b). A complete automated processing including cortical and subcortical labelling using the Desikan-Killiany atlas was performed on each subject. Then, the hippocampal subfields were accessed using the Freesurfer v6.0.0, sub-dividing the hippocampus into subfields namely hippocampal tail(tail), subiculum(SUB), cornu ammonis 1(CA1), hippocampal fissure(fissure), presubiculum (PSUB), parasubiculum (ParaSUB), molecular layer(ML), granule cells/molecular layer/dentate gyrus (GCMLDG), cornu ammonis 3(CA3), cornu ammonis 4(CA4), fimbria and hippocampal-amygdala transition area(HATA) (Iglesias et al., 2015).

PET imaging

Subjects underwent a PET scan 90 minutes after intravenous injection of 300 MBq ^{18}F-Florbetaben (F-18) using a dedicated Discovery ST PET-CT scanner (General Electric Medical Systems, Milwaukee, WI, USA). Non-contrast-enhanced CT scans were used for attenuation correction with technical parameters of 120 Kvp, 10-130 mAs, 8 slices, helical and 3.79 mm slice thickness. PET and CT scan data were reconstructed using ordered subset expectation maximization (OSEM) after attenuation correction with 2 iterations and 21 subsets. A Gaussian filter was applied with 5.14 mm FWHM to reconstruct a 128 × 128 matrix with 3.27-mm slice thickness.

PET image data processing

PET images were assessed according to a predefined regional cortical tracer uptake (RCTU) scoring system (1=no uptake, 2=minor uptake, 3=pronounced uptake) for 4 brain regions (frontal cortex, posterior cingulate, lateral temporal cortex, parietal cortex). Details of a three-grade scoring system using RCTU scores for the amyloid plaque load are previously provided (Barthel et al., 2011). For the PiB-PET images, the mean retention value of the global cortical region of interest (ROI) was used to define the global cerebral Aβ deposition as amyloid-positive if the mean standard value uptake ratios (SUVR) > 1.4 in at least one of the ROIs including frontal, lateral parietal, lateral temporal or posterior cingulate-precuneus (Choi et al., 2017).

Statistical analysis

All statistical analysis was performed using IBM SPSS Statistics (Version 23.0. Armonk, NY: IBM Corp.) One-way Analysis Of Variance (ANOVA) and Bonferroni post hoc correction for multiple comparisons was used for continuous demographic variables and Chi-squared test was performed on categorical demographic variables. Differences among the diagnostic groups were tested using Analysis of covariance (ANCOVA) and when the ANCOVA was significant (greater than the value of adjusted

multiple comparison, Table 1&2), pairwise Bonferroni post hoc was applied to check the between groups differences. We considered *p-values* <0.05 as significant. The analysis was two-tailed and controlled for covariates age, sex, years of education and estimated total intracranial volume. All analyses were separately performed for the left and right hemispheres.

2.3. Results

No significant differences in terms of age ($F_{5, 478} = 1.29, p = 0.26$) and gender ($\chi^2$ *test:* $\chi^2 = 6.60, p = 0.25$) were observed among the groups. Levels of education ($F_{5, 478} = 2.54, p = 0.02$. *post hoc: CIND versus ADD, 0.01, others were insignificant*) was significantly different when compared among all the groups although pairwise comparison revealed that the difference was only specific to CIND and ADD groups. The MMSE scores were significantly different between the groups ($F_{5, 478} = 73.44, p = 1.08E\text{-}56$). However, the post hoc analyses showed that the scores were not different between Asymptomatic AD & NC, Prodromal AD & CIND and non-AD dementia & ADD groups (Table 2).

Group comparisons of the six groups showed that hippocampal fissure was not significantly different between the groups (after adjusting for Bonferroni correction, $p < 9.61\text{-}4$). In addition, the bilateral parasubiculum, left CA3 and right fimbria did not show any significant volume differences in the Asymptomatic AD and Prodromal AD. Left fimbria and right CA3 did

not show any significant atrophy between the Prodromal AD and ADD. The percentile volume loss was high in prodromal AD to Alzheimer's disease dementia stage than preclinical AD to prodromal AD stage. Predominantly, there was higher percentile volume loss in the left hemisphere than right hemisphere (Table S1).

Subfield volumes in NC & Asymptomatic AD were not significantly different from each other. We observed left-right hemispheric differences in both the groups, with significantly larger right hemisphere volumes than the left hemisphere, except PSUB, ParaSUB, fimbria and HATA (Table S2). In these regions, the volumes of the right were smaller than the left. However, in Asymptomatic AD they were not statistically significant except fimbria. The asymmetries were high in the NC (β-amyloid negative) than Asymptomatic AD (β-amyloid positive). In comparison to other subfield, the left-right ParaSUB volumes in NC and Asymptomatic AD were weakly correlated (Table S3).

Bilateral volumes of hippocampal tail, CA1, ML, GCMLDG, CA4 and right CA3 were significantly different between CIND & Prodromal AD with larger volumes in CIND than Prodromal AD (Table S1). Left-right hemispheric asymmetries were significantly high in CIND (β-amyloid negative) than Prodromal AD (β-amyloid positive). All other subfield except PSUB, ParaSUB, HATA and fimbria (Table S2) had larger right hemisphere

volumes. Similar to NC & Asymptomatic AD, the left-right ParaSUB volumes in CIND and Prodromal AD were moderately correlated (Table S3).

Non-AD dementia had significantly larger volumes than ADD in bilateral tail, SUB, PSUB and left ML (Table S1 & S1a). Subfield other than PSUB, ParaSUB, HATA and fimbria (Table S2) had larger right hemisphere volumes than the left. Inconsistent with the Normal controls & Asymptomatic AD and Cognitive impairment that are not dementia & Prodromal AD, the left-right hemispheric asymmetry were lower in non-AD dementia (β-amyloid negative) than ADD (β-amyloid positive) (Table S2). In addition, the ParaSUB left-right hemispheric volumes were weakly correlated in ADD and moderately correlated in non-AD dementia (Table S3).

2.4. Discussion

Amyloid plaques and the neurofibrillary tangles define AD as unique among the other dementias but are not enough to confirm the presence of AD. Without the neurodegeneration which provides vital pathological staging, the differences between the plaques and tangles would not be formally captured. Furthermore, the combination of abnormal sMRI with an abnormal amyloid imaging provides significantly powerful prediction of

future cognitive impairment than an abnormal amyloid imaging alone (Jack et al., 2018).

The current study to the best of our knowledge is the first to investigate the differences in neurodegeneration of the hippocampal subfield in groups of participants classified based on β-amyloid burden and cognitive spectrum from cognitively unimpaired to mild cognitively impaired to severe cognitive impairment. We studied the hemispheric asymmetry and correlation between the individual hemispheric subfield volumes. The trajectory of AD associated atrophy is asymmetrical and starts around the CA1-subiculum regions and propagates outward gradually to other regions, finally reaching the parasubiculum, CA3 and fimbria regions in the late prodromal AD stages.

Differential volume loss among groups

The group comparisons of the subjects showed that all the subfields were significantly different from each other bilaterally, except the hippocampal fissure. However, the pairwise comparison elucidated that certain subfield volumes of few groups were rather not statistically significantly different. In prior studies, subjects with abnormal levels of β-amyloid at baseline, in cognitively normal, subjects with mild cognitive impairment and AD dementia were inclined to greater cognitive and global deterioration compared to peers without abnormal β-amyloid levels

(Doraiswamy et al., 2014, Knopman et al., 2013, Knopman et al., 2015). Approximately 10-30% of cognitively normal individuals have abnormal levels of β-amyloid suggesting a biological relevance of slight β-amyloid elevations in normal aging (Mormino et al., 2012, Rowe et al., 2010). In the present study, we found that none of the subfield showed significant difference between the NC & Asymptomatic AD groups. Neurodegeneration is believed to cause cognitive dysfunction that in turn is expected to be mediated by the deposition of β-amyloid (Mormino et al., 2009). Abnormal levels of β-amyloid are not sufficient to cause apparent cognitive symptoms (Jack et al., 2009). Thus, the current stage might be early for any apparent volume loss; a longitudinal study of the NC & Asymptomatic AD groups might provide a very clear picture of the underlying mechanisms. Our findings here are in line with earlier study showing β-amyloid deposition in cognitively unimpaired subjects (Jagust et al., 2010, Mormino et al., 2012, Rowe et al., 2010). Furthermore, as with the final model of temporal ordering of the biomarkers in the Dominantly Inherited Alzheimer Network (DIAN) study (Bateman et al., 2012), there was a trend level increase in the Asymptomatic AD than the Normal controls.

When we compared the NC and Asymptomatic AD groups to CIND, almost all the subfield volume differences were statistically insignificant, bilaterally. However, it is shown that the hippocampal atrophy can act as

strong predictor of AD progression and capable of discriminating mild cognitively impaired from cognitively normal (Henneman et al., 2009). Interestingly, this was the case exclusively when both NC and Asymptomatic AD groups were compared to Prodromal AD where most of the subfield showed statistically significant difference in volumes, bilaterally. This may indicate that the Prodromal AD might be the transitional stage involved in the AD continuum and the differences in the subfield volumes might be useful to classify subjects with mild cognitive impairment into Prodromal AD and CIND even prior to the β-amyloid imaging. A more extensive study might help confirm this and understand the underlying mechanisms. To the best of our knowledge this evaluation has not been reported elsewhere.

The NC and Asymptomatic AD groups were compared to the ADD and non-AD dementia where there was a highly significant difference in all groups for all the subfield, clearly differentiating the normal controls from demented subjects in line with numerous studies reported earlier (West et al., 1994, Frisoni et al., 2008, Du et al., 2001).

A longitudinal observational study with serial imaging (Knopman et al., 2015) reported no significant differences in adjusted hippocampal volume between the amyloid positive and negative groups with mild cognitive impairment while another prospective cohort study (Landau et al., 2016) has shown significantly higher glucose metabolism and larger

hippocampal volume in the CIND than the Prodromal AD. In the current study, when we compared mild cognitively impaired subject groups Prodromal AD and CIND, we observed no significant volume difference of the subicular complex (SUB, PSUB and ParaSUB) bilaterally but there was atrophy in bilateral tail, CA1, ML, GC-ML-DG, CA4 and right CA3. This is partly in line with the earlier study, and the discrepancies may be due to the differences in the analyses (hippocampal subfield and whole hippocampal volume) and use of different population in our study.

We then compared the Prodromal AD & CIND with ADD & non-AD dementia groups. There were clear differences when CIND was compared with ADD and non-AD dementia. The CIND might be the cognitive impairment resulting from normal aging process, metabolic disturbance, substance abuse and head trauma (Harada et al., 2013, Albert et al., 2011). Bilateral ParaSUB, left fimbria and right CA3 did not show volume loss while comparing Prodromal AD & ADD suggesting that these regions are affected only in the late AD stages located away from the suspected pathological initiation sites, the CA1 and the subiculum (Apostolova et al., 2006, Devanand et al., 2012, Wang et al., 2006).

Finally, comparison of ADD and non-AD dementia showed differences in the bilateral SUB, PreSUB, tail and left ML suggesting that the volume atrophy in ADD might be severe than non-AD dementia or certain

other types of dementia (Delli Pizzi et al., 2016). All other subfield showed no significant differences. A portion of subjects in the non-AD dementia group has been shown to demonstrate Aβ positivity in longitudinal study (Gordon et al., 2016).

Majority of the subfield volume losses in the Prodromal AD were found to be severe compared to either normal controls or the Asymptomatic AD. Although, it was not the case with CIND suggesting the Prodromal AD might be the transitional stage between Asymptomatic AD and ADD. Thus the progression of AD might be NC to Asymptomatic AD to Prodromal AD to ADD. This study shows the importance of separating the Aβ positive from the Aβ negative.

In cognitively unimpaired and mild cognitively impaired, Aβ-negative showed higher hemispheric volume difference than Aβ-positive. On the contrary, in severe cognitively impaired the Aβ-positive (ADD) showed higher hemispheric volumetric difference than Aβ-negative (non-AD dementia) (Delli Pizzi et al., 2016).

Selective vulnerability among subfield

Neuropathological studies have reported that AD continuum is a complex and ordered sequential process involving neuronal loss around the CA1-subiculum regions with the atrophy beginning at the anterior CA1-subiculum regions subsequently progressing toward other subfield (Corder et

al., 2000, Kerchner et al., 2012, Apostolova et al., 2006, Devanand et al., 2012). Other study reported a presubicular-subicular complex atrophy in the earliest stages of AD (Carlesimo et al., 2015). Studies have also reported bilateral atrophy in the cornu ammonis and subiculum in AD than controls (Chow et al., 2012, Firbank et al., 2010, Mak et al., 2016). Similar findings have also been reported in structural imaging studies with bilateral atrophy in subiculum, CA1 and CA2-3 regions (Mak et al., 2016, Chow et al., 2012). In line with the previous findings, in the current study we observed atrophy in both the CA1 and subiculum regions between the cognitively unimpaired groups and Prodromal AD. Additionally, atrophy in other subfield was also observed between the cognitively unimpaired groups and Prodromal AD. Although, bilateral parasubiculum, left CA3 and right fimbria situated away from the CA1-subiculum regions are seen to be preserved till the late AD stages. Contrary to the earlier studies right CA3 and left fimbria were atrophied in the early AD stage indicating asymmetrical atrophy patterns. Parasubiculum is a transitional area sandwiched between the presubiculum and entorhinal area (Duvernoy, 2005) and postulated to play an vital role in the spatial navigation and the integration of head-directional information (Taube Jeffrey, 2004). Fimbria extend to fornix, the white matter of the brain and the CA3 is expected to be the largest in the hippocampus (Fogwe and Mesfin, 2018). The parasubiculum and CA3 are regions situated far from the

suspected atrophy initiation sites the CA1 or subiculum. The atrophy of these sites might suggest terminal stages of the disease propagation which later spreads to other regions.

Earlier study has reported left less than right asymmetrical hippocampal volume. Additionally, significant left hippocampal volume loss over right (Müller et al., 2005). We found that the volume losses in the left hemisphere were found to be severe in comparison with the right hemisphere with asymmetrical pattern of atrophy. Similarly, the early stage atrophies of the left fimbria and the right CA3 than their respective other hemispherical half that shows a difference in the atrophy patterns (Mesulam et al., 2014). These hemispheric volume differences are seen in almost all subfield with larger right hemisphere volumes except PSUB, ParaSUB and HATA. Irrespective of the groups, especially in ParaSUB, there was weak correlation of left-right hemispheric volumes (this weak correlation was statistically insignificant in Asymptomatic AD).

In line with prior studies, the mean age of the participants in our study was around the early seventies. Further targeted studies on early age group subjects for clear and better understanding of the pathophysiological mechanisms are required. Since, the hallmarks of the Alzheimer's disease, the amyloid beta plaques form long before the clinical symptoms are seen; subjects aged around the sixth decade or later might be too late for any

diagnostic studies. In addition, the delayed atrophy of specific subfields till the later stages of Alzheimer's disease progression warrants detailed longitudinal studies focused on these subfields to understand the preventive mechanisms. The current study confirms the selective vulnerability of hippocampal subfields in the prodromal AD subjects over the CIND.

In conclusion, the results establish that the early deposition of the β-amyloid as seen in cognitively normal subjects may not be accompanied by the neurodegeneration. Additionally, the subfield volumes to some extent may be helpful in determining individuals with mild cognitive impairment due to Alzheimer.

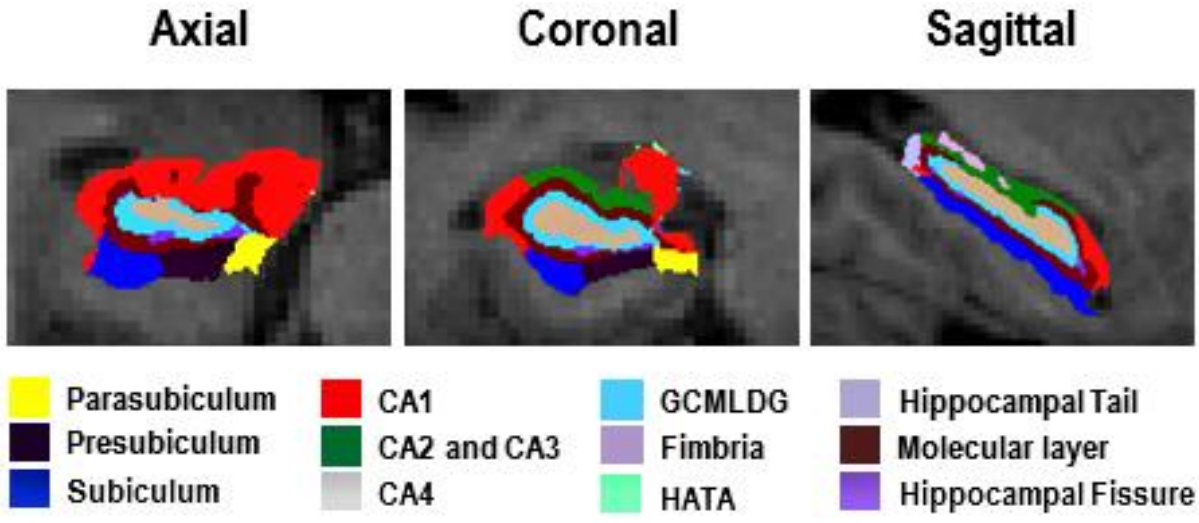

Figure 10. An illustration of neuro-anatomically distinct non-homogenous hippocampal subfields as segmented by the novel method used in the study. CA – cornu ammonis, GCMLDG – granule cell layer of dentate gyrus, HATA – hippocampus-amygdala-transition area

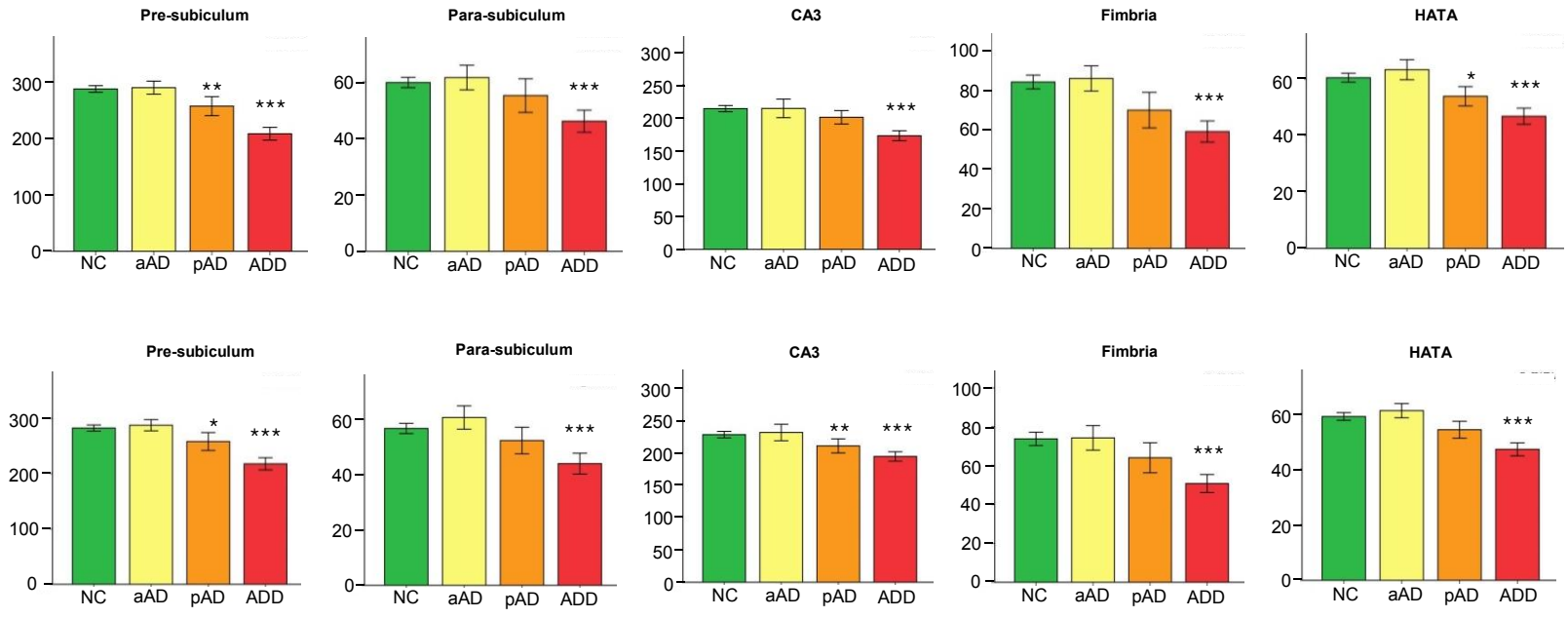

Figure 11. Hippocampal subfield volumes in Normal Controls, Asymptomatic AD, Prodromal AD and Alzheimer's disease Dementia. Error bar indicates two standard error. Upper panel: left hemisphere volume differences. Lower panel: right hemisphere volume differences. Abbreviations: NC, Normal controls; aAD, Asymptomatic Alzheimer's disease; pAD, Prodromal Alzheimer's disease; ADD, Alzheimer's Disease Dementia; All statistical significance with respect to normal controls; *- $p<0.05$; **- $p<0.01$; ***- $p<0.001$

Table 2. Study participants were grouped based on β-amyloid burden and cognitive status

β-amyloid burden	Cognitively unimpaired	Mild cognitive impairment	Severe cognitive impairment
Positive	Asymptomatic AD (n=34)	Prodromal AD (n=34)	Alzheimer's disease Dementia (ADD, n=70)
Negative	Normal controls (NC, n=192)	Cognitive impairment that are not dementia (CIND, n=118)	non-AD dementia (n=30)

Table 3. Demographic characteristics of study participants

	Asymptomatic AD	Normal controls (NC)	Prodromal AD	CIND	Alzheimer's disease dementia (ADD)	Non-AD dementia
Number of subjects (n)	34	192	34	118	70	30
Age[a,b]	73.80±4.21	71.95±5.30	74.17±6.11	72.50±6.96	72.18±6.92	73.76±6.48
Male percentage (%) [c]	47.05	46.35	67.64	43.22	48.57	50
Level of education (years) [a,d]	8.79±5.75	9.32±5.50	8.82±4.93	9.66±5.15	7.48±5.03	9.13±6.02
MMSE [a,e]	27.41±2.09	27.43±2.03	25.23±3.14	25.17±3.39	19.41±5.73	19.06±7.86

Values are expressed as mean ± standard deviation (SD).

Key: AD, Alzheimer's disease; ANOVA, analysis of variance; MMSE, Mini Mental State Examination

[a] The *p*-values were calculated using general linear model; Bonferroni post hoc test was also performed when F-test was significant.

[b] Main interaction among groups: $F_{5, 478} = 1.29$, $p = 0.26$. *(Age)*

[c] The *p*-value was calculated using the χ^2 test: $\chi^2 = 6.60$, $p = 0.25$. *(Gender)*

[d] Main interaction among groups: $F_{5, 478} = 2.54$, $p = 0.02$. Post hoc: CIND versus ADD, 0.01, others were insignificant. *(Education)*

[e] Main interaction among groups: $F_{5, 478} = 73.44$, $p = 1.08E\text{-}56$. post hoc: NC versus Asymptomatic AD, 1.00; NC versus Prodromal AD, 8.99E-3; NC versus ADD, 5.77E-45; NC versus CIND, 3.46E-7; NC versus non-AD dementia, 1.61E-29; Asymptomatic AD versus Prodromal AD, 0.04; Asymptomatic AD versus ADD, 2.85E-24; Asymptomatic AD versus CIND, 2.58E-3; Asymptomatic AD versus non-AD dementia, 2.29E-20; Prodromal AD versus ADD, 1.90E-12; Prodromal AD versus CIND, 1.00; Prodromal AD versus non-AD dementia, 5.93E-11; CIND versus ADD, 8.71E-22; CIND versus non-AD dementia, 1.14E-15; ADD versus non-AD dementia, 1.00. *(MMSE)*

Table 4. Volume (mm^3) for left and right hippocampal subfields

Regions	Asymptomatic AD	NC	Prodromal AD	CIND	ADD	non-AD dementia	*ANCOVA (F, p-value)*
L-Tail	477.84±73.85	472.28±68.34	418.37±68.78	462.28±68.43	367.24±68.69	423.95±78.52	***29.73, 3.03E-26***
L-Sub	424.64±49.35	417.85±56.92	369.83±63.23	401.40±60.71	308.11±66.61	347.25±72.95	***46.39, 6.44E-39***
L-CA1	614.49±81.20	598.89±75.10	544.91±72.45	583.79±74.48	477.85±92.31	511.09±98.12	***34.57, 4.39E-30***
L-Fissure	172.10±34.43	160.11±27.90	159.41±24.29	162.21±29.12	149.88±33.57	154.83±34.00	3.13, 8.59E-3
L-PSUB	289.84±33.58	287.52±40.76	257.19±48.99	272.08±44.17	208.21±47.41	237.46±53.27	***43.68, 5.82E-37***
L-Para SUB	61.55±12.74	59.79±12.68	55.16±17.36	56.40±13.78	46.09±16.36	48.78±17.24	***11.57, 1.48E-10***
L-ML	546.98±63.55	539.50±65.19	482.60±66.31	522.99±68.09	408.85±77.50	449.87±87.82	***52.67, 2.52E-43***
L-GCMLDG	296.35±39.54	295.08±36.86	263.17±35.50	287.45±36.80	229.96±40.92	245.29±47.92	***44.33, 1.98E-37***
L-CA3	214.03±41.08	213.70±32.77	200.53±29.85	210.59±27.94	172.54±31.82	178.19±37.09	***24.35, 8.15E-22***
L-CA4	259.05±35.00	257.03±30.88	231.55±29.38	251.07±30.58	202.21±35.73	215.96±42.23	***43.16, 1.41E-36***
L-Fimbria	85.99±18.62	84.19±24.14	69.97±26.30	81.24±25.53	59.14±22.42	63.84±25.77	***14.60, 2.60E-13***
L-HATA	63.29±10.32	60.46±10.89	53.89±9.95	57.78±9.66	46.82±11.96	46.62±10.91	***25.40, 1.07E-22***
R-Tail	513.29±74.27	505.78±68.02	461.81±73.33	498.45±70.93	413.57±73.19	462.34±84.05	**21.06, 5.16E-19**

R-Sub	441.39±44.07	432.65±56.53	390.26±62.43	414.59±61.67	329.74±68.34	365.66±73.24	**39.00,1.74E-33**
R-CA1	655.64±75.23	641.90±81.02	592.31±77.94	627.89±81.62	533.81±95.01	555.63±90.33	**25.74, 5.68E-23**
R-Fissure	188.08±29.16	178.30±33.36	178.40±34.44	177.75±30.78	181.48±38.14	172.64±33.38	0.93, 0.45
R-PSUB	287.46±29.52	282.33±38.26	258.08±47.01	268.26±39.84	217.71±46.03	238.89±40.17	**33.00, 7.43E-29**
R-Para SUB	60.63±12.27	56.68±12.72	52.31±14.01	54.45±13.15	43.96±15.75	47.85±12.89	**12.41, 2.51E-11**
R-ML	575.95±61.62	567.40±69.10	516.56±69.68	550.98±72.96	449.71±79.22	481.45±81.13	**39.56, 6.63E-34**
R-GCMLDG	311.51±41.24	307.42±40.85	281.64±38.63	302.33±40.69	252.92±38.89	261.94±45.51	**28.88, 1.47E-25**
R-CA3	231.05±37.00	227.71±34.42	210.36±31.59	225.64±32.92	194.06±30.42	196.48±36.07	**16.61, 4.06E-15**
R-CA4	272.52±35.67	268.15±33.52	246.65±31.58	264.53±33.82	222.69±33.48	231.73±39.16	**29.13, 9.25E-26**
R-Fimbria	74.23±18.37	73.72±23.69	64.02±22.51	68.86±23.97	50.77±19.31	55.49±20.87	**13.50, 2.55E-12**
R-HATA	61.07±7.45	58.96±9.53	54.20±8.87	56.58±9.04	47.14±9.79	49.75±9.54	**21.61, 1.74E-19**

Values are expressed as mean ± standard deviation (SD); Bold characters indicate significant results.

Key: L-, left; R-, right; ADD, Alzheimer's disease dementia; Asymptomatic Alzheimer's disease; Prodromal Alzheimer's disease ; CIND, cognitive impairment that are not dementia; ANCOVA, analysis of covariance; Tail, hippocampal tail; Sub, subiculum; CA, cornu ammonis; PSUB, presubiculum; ParaSUB, parasubiculum; ML, molecular layer; GCMLDG – granule cell layer of dentate gyrus, HATA – hippocampus-amygdala-transition area.

[a]ANCOVA followed by Bonferroni correction was carried out to test the differences among groups (adjusting for covariates age, gender, level of education and total intracranial volume. adjustment for multiple comparison: $p = 0.05/13$ structures/4 groups = 9.61E-4). When the ANCOVA was significant, pairwise Bonferroni post hoc was applied. Whole hippocampus data not shown.

Table 4A. Bonferroni pairwise post hoc

Region	NC vs Prodromal AD	NC vs ADD	NC vs non-AD dementia	Asymptomatic AD vs Prodromal AD	Asymptomatic AD vs ADD	Asymptomatic AD vs CIND	Asymptomatic AD vs non-AD dementia	Prodromal AD vs ADD	Prodromal AD vs CIND	CIND vs ADD	CIND vs non-AD dementia	ADD vs non-AD dementia
L-Tail	**1.16E-3**	**1.29E-24**	**0.03**	**2.37E-3**	**1.32E-14**	1.00	**0.02**	**1.45E-3**	**0.01**	**3.35E-19**	0.18	**1.85E-4**
L-Sub	**3.17E-4**	**1.13E-35**	**2.02E-7**	**3.10E-4**	**6.56E-22**	0.25	**9.66E-7**	**1.00E-6**	0.05	**3.02E-25**	**1.67E-4**	**2.97E-3**
L-CA1	**6.66E-4**	**1.09E-25**	**6.63E-7**	**2.09E-4**	**4.90E-17**	0.43	**7.50E-7**	**1.11E-3**	**0.01**	**3.21E-19**	**5.10E-5**	0.26
L-Fissure	NA	NA	NA	NA	NA	NA	NA	NA	NA	NA	NA	NA
L-PSUB	**6.99E-3**	**3.05E-35**	**5.36E-7**	**9.78E-3**	**1.66E-20**	0.17	**8.00E-6**	**3.48E-8**	1.00	**1.51E-22**	**2.33E-3**	**2.05E-3**
L-Para SUB	0.84	**8.56E-10**	**3.10E-3**	0.54	**4.00E-6**	0.98	**6.49E-3**	0.08	1.00	**2.60E-5**	0.15	1.00
L-ML	**4.70E-5**	**1.24E-38**	**1.58E-9**	**8.20E-5**	**1.69E-23**	0.48	**3.07E-8**	**7.11E-7**	**6.34E-3**	**8.04E-29**	**1.00E-6**	**9.20E-3**
L-GCML DG	**1.40E-5**	**3.43E-32**	**7.88E-10**	**2.06E-4**	**3.82E-18**	1.00	**1.68E-7**	**2.89E-4**	**1.02E-3**	**1.77E-24**	**2.22E-7**	0.26
L-CA3	0.11	**3.47E-18**	**4.96E-7**	0.29	**1.31E-9**	1.00	**5.50E-5**	**1.47E-3**	0.26	**4.80E-15**	**4.00E-6**	1.00

L-CA4	**3.40E-5**	**2.01E-31**	**2.47E-9**	**2.68E-4**	**4.66E-18**	1.00	**2.37E-7**	**2.39E-4**	**1.46E-3**	**2.84E-24**	**3.65E-7**	0.23
L-Fimbria	0.06	**1.48E-11**	**1.61E-3**	0.06	**3.60E-7**	1.00	**3.60E-3**	0.26	0.32	**1.53E-8**	**0.01**	1.00
L-HATA	**0.02**	**4.81E-17**	**6.59E-9**	**1.64E-3**	**5.15E-13**	**0.04**	**3.91E-9**	**0.01**	0.96	**1.77E-10**	**9.00E-6**	1.00
R-Tail	**7.87E-3**	**1.08E-17**	0.09	0.01	**1.86E-10**	1.00	0.08	**0.03**	**0.03**	**2.67E-14**	0.25	**7.45E-3**
R-Sub	**2.09E-3**	**7.01E-31**	**2.00E-6**	**1.26E-3**	**3.28E-19**	0.16	**4.00E-6**	**7.00E-6**	0.26	**1.10E-20**	**1.29E-3**	**0.01**
R-CA1	**1.87E-3**	**5.31E-19**	**3.00E-6**	**1.42E-3**	**3.03E-12**	1.00	**1.00E-5**	**0.03**	**0.02**	**2.87E-14**	**1.06E-4**	1.00
R-Fissure	NA	NA	NA	NA	NA	NA	NA	NA	NA	NA	NA	NA
R-PSUB	**0.03**	**3.65E-27**	**5.00E-6**	**0.02**	**1.44E-16**	0.10	**1.80E-5**	**4.00E-6**	1.00	**2.46E-16**	**9.03E-3**	**0.04**
R-Para SUB	0.85	**4.57E-10**	**0.01**	0.11	**7.27E-8**	0.32	**2.54E-3**	0.06	1.00	**3.00E-6**	0.21	1.00
R-ML	**4.28E-4**	**8.37E-30**	**4.06E-8**	**5.84E-4**	**3.84E-18**	0.71	**4.76E-7**	**8.40E-5**	**0.02**	**9.22E-22**	**1.20E-5**	0.14
R-GCML DG	**1.16E-3**	**1.11E-20**	**2.66E-7**	**1.95E-3**	**1.36E-12**	1.00	**3.00E-6**	**0.02**	**6.74E-3**	**8.80E-17**	**3.00E-6**	1.00
R-CA3	**7.73E-3**	**4.53E-11**	**4.40E-5**	**0.01**	**8.74E-7**	1.00	**3.05E-4**	1.00	**0.01**	**1.02E-9**	**8.60E-5**	1.00
R-CA4	**6.47E-4**	**1.04E-20**	**8.07E-7**	**8.74E-4**	**6.37E-13**	1.00	**5.00E-6**	**0.03**	**2.65E-3**	**2.71E-17**	**5.00E-6**	1.00
R-Fimbria	1.00	**7.85E-12**	**3.39E-3**	1.00	**4.50E-7**	1.00	**8.73E-3**	**6.30E-3**	1.00	**5.03E-7**	0.12	1.00
R-HATA	0.08	**5.85E-17**	**4.10E-5**	0.01	**5.45E-12**	0.13	**1.90E-5**	**5.07E-3**	1.00	**1.63E-10**	**7.10E-3**	1.00

Values are expressed as pairwise comparison *p-values*; Bold characters with $p<0.05$ indicate significant results.

Key: NA, Not applicable; L-, left; R-, right.

Table 5. Comparison of hemispheric differences with paired t-test

Regions	NC (t, *p-value*)	Asymptomatic AD (t, *p-value*)	CIND (t, *p-value*)	Prodromal AD (t, *p-value*)	non-AD dementia (t, *p-value*)	ADD (t, *p-value*)
Tail	***-9.18, 7.11E-17***	***-4.97, 2.00E-5***	***-9.57, 2.18E-16***	***-5.95, 1.00E-6***	***-3.87, 5.58E-4***	***-8.81, 6.59E-13***
Sub	***-5.38, 2.14E-7***	***-2.91, 6.37E-3***	***-4.99, 2.00E-6***	***-3.51, 1.28E-3***	***-2.53, 0.01***	***-3.79, 3.15E-4***
CA1	***-10.85, 1.06E-21***	***-6.24, 4.67E-7***	***-10.23, 5.96E-18***	***-5.74, 2.00E-6***	***-4.43, 1.20E-4***	***-6.34, 1.96E-8***
Fissure	***-9.79, 1.27E-18***	***-4.29, 1.45E-4***	***-6.91, 2.59E-10***	***-4.31, 1.38E-4***	***-5.72, 3.00E-6***	***-8.41, 3.50E-12***
PSUB	***2.24, 0.02***	*0.44, 0.65*	*1.61, 0.10*	*-0.18, 0.85*	*-0.22, 0.82*	*-1.88, 0.06*
ParaSUB	***3.09, 2.26E-3***	*0.34, 0.73*	*1.55, 0.12*	*1.21, 0.23*	*0.39, 0.69*	*0.90, 0.36*
ML	***-9.13, 9.32E-17***	***-4.61, 5.60E-5***	***-8.13, 5.05E-13***	***-5.08, 1.50E-4***	***-3.77, 7.28E-4***	***-5.87, 1.33E-7***
GCMLDG	***-6.91, 6.95E-11***	***-3.71, 7.49E-4***	***-7.38, 2.41E-11***	***-4.86, 2.70E-5***	***-3.11, 4.10E-3***	***-6.85, 2.46E-9***
CA3	***-7.85, 2.88E-13***	***-4.56, 6.60E-5***	***-7.30, 3.61E-11***	***-2.48, 0.01***	***-4.14, 2.73E-4***	***-7.26, 4.31E-10***
CA4	***-7.09, 2.47E-11***	***-4.10, 2.50E-4***	***-7.73, 3.99E-12***	***-4.72, 4.10E-5***	***-3.37, 2.10E-3***	***-6.76, 3.55E-9***
Fimbria	***7.42, 3.67E-12***	***4.14, 2.22E-4***	***7.27, 4.23E-11***	*1.64, 0.11*	***2.23, 0.03***	***4.01, 1.47E-4***
HATA	***2.27, 0.02***	*1.38, 0.17*	*1.88, 0.06*	*-0.22, 0.82*	***-2.70, 0.01***	*-0.22, 0.81*

Values are expressed as t-statistics and respective *p-values*.

Bold characters with $p<0.05$ indicate significant results.

Table 6. Correlation between the two hemispheres

Regions	NC (r, *p-value*)	Asymptomatic AD (r, *p-value*)	CIND (r, *p-value*)	Prodromal AD (r, *p-value*)	non-AD dementia (r, *p-value*)	ADD (r, *p-value*)
Tail	***0.72, 1.37E-32***	***0.84, 4.05E-10***	***0.82, 8.10E-31***	***0.82, 2.31E-9***	***0.77, 3.84E-7***	***0.80, 2.19E-17***
Sub	***0.77, 1.21E-39***	***0.74, 3.66E-7***	***0.89, 1.92E-41***	***0.85, 1.22E-10***	***0.85, 2.30E-9***	***0.75, 7.41E-14***
CA1	***0.75, 1.03E-36***	***0.88, 5.38E-12***	***0.82, 2.07E-30***	***0.79, 1.59E-8***	***0.83, 1.11E-8***	***0.69, 3.76E-11***
Fissure	***0.66, 1.90E-25***	***0.77, 5.55E-8***	***0.66, 1.17E-16***	***0.66, 1.60E-5***	***0.87, 3.31E-10***	***0.62, 8.66E-9***
PSUB	***0.67, 1.42E-26***	***0.52, 1.54E-3***	***0.81, 1.87E-29***	***0.82, 2.74E-9***	***0.76, 8.24E-7***	***0.59, 6.36E-8***
ParaSUB	***0.40, 8.37E-9***	*0.21, 0.21*	***0.49, 1.34E-8***	***0.64, 4.30E-5***	***0.67, 4.70E-5***	***0.25, 0.03***
ML	***0.80, 1.32E-44***	***0.82, 1.30E-9***	***0.86, 5.90E-36***	***0.83, 6.95E-10***	***0.85, 1.61E-9***	***0.72, 1.28E-12***
GCMLDG	***0.80, 2.04E-44***	***0.82, 1.61E-9***	***0.84, 2.36E-33***	***0.82, 1.98E-9***	***0.80, 8.09E-8***	***0.75, 4.69E-14***
CA3	***0.72, 3.21E-33***	***0.84, 2.02E-10***	***0.74, 8.04E-22***	***0.71, 2.00E-6***	***0.78, 3.42E-7***	***0.68, 6.69E-11***
CA4	***0.77, 8.45E-40***	***0.85, 1.42E-10***	***0.83, 1.57E-31***	***0.81, 4.12E-9***	***0.80, 8.12E-8***	***0.73, 4.90E-13***
Fimbria	***0.66, 4.72E-26***	***0.60, 1.74E-4***	***0.72, 2.24E-20***	***0.63, 5.40E-5***	***0.63, 1.79E-4***	***0.65, 5.19E-10***
HATA	***0.60, 9.43E-21***	***0.48, 3.63E-3***	***0.73, 6.56E-21***	***0.64, 3.50E-5***	***0.81, 3.93E-8***	***0.43, 1.80E-4***

Values are expressed as correlation co-efficient values '*r*' and respective *p-values*.

Bold characters with $p<0.05$ indicate significant results.

CHAPTER 3

Hippocampal subfield volumes allow better statistical modelling for the prediction of Alzheimer's disease than hippocampal volumes

Abstract

Alzheimer's disease is gradually emerging into a threatening socially disruptive condition of the aging population. Identification of subjects who are at risk of developing Alzheimer's disease (AD), by the time the pathological hallmarks passively present themselves or at least before the clinical symptoms actively exhibits themselves, with sufficient accuracy will have great potential to target the right subjects for clinical trials. Hippocampus is among the earliest regions affected by the process of healthy cognitive aging and pathological aging alike. Hippocampus is a heterogeneous structure with distinct subfields. Thus, we investigated the AD prediction power of the hippocampal subfield volumes against that of the overall hippocampal volume. Additionally, we investigated the alterations in the predictive performance with the addition of various factors such as age, gender, level of education and total intracranial volume. We used logistic regression and the results showed that the subfield volumes had better performance than hippocampal volume across different models used. The additional factors such as age and gender had only minor change in the performance.

Keywords: Alzheimer's disease, MRI, hippocampal subfield volumes, cognitive aging and pathological aging

3.1. Introduction

The aging brain undergoes structural and functional changes via a variety of processes which is linked to gradual changes in global and regional measures among distant brain regions. Basic and higher levels of cognitive functioning both require the cooperation and coordination of multiple brain regions. Identifying and understanding the distributed patterns of brain structures supporting the preeminent functions of the brain are challenging. Understanding these brain structures is the first step in understanding the underlying mechanisms of various age related disorders and changes. With the increased worldwide prevalence of Alzheimer's disease and other age related disorders, there is a sense of urgency in identifying valid biomarkers which can help in comprehending the healthy aging process and with the early detection of age associated disorders, thereby helping in the therapeutic interventions and further trials (Jack et al., 2018, McKhann et al., 2011). Obtaining the well-established hallmarks of the Alzheimer's disease, the beta amyloid plaques and the neurofibrillary tangles are relatively challenging and thus using the neuropsychological battery, structural magnetic resonance imaging and statistical and computational procedures for fundamental questions before a detailed study has been done in earlier research.

Structural magnetic resonance imaging (sMRI) provides a wide variety of measures such as cortical thickness, cortical surface area, cortical and subcortical volumes among others, distributed across the brain. Thus, providing a myriad sets of data which may assist in an array of basic research problems and thereby useful for

clinical applications. Numerous studies have used the voxel based morphometry in the statistical modelling and classification of subjects (Hinrichs et al., 2011, Adaszewski et al., 2013, Hinrichs et al., 2009, Aksu et al., 2011). Similarly, the other morphometries obtained from the sMRI like the cortical and subcortical volumes (Kohannim et al., 2010, McEvoy et al., 2011) and cortical thickness, surface area and hippocampal morphology (Aguilar et al., 2013, Costafreda et al., 2011, Cuingnet et al., 2011, Vemuri et al., 2008, Ewers et al., 2012) have also been used for analysis. Though, many studies have been performed using the global measures of cortical volume, cortical surface area and cortical thickness. Many detailed studies on one of the first regions to be affected in healthy cognitive aging process and pathologically abnormal aging, the hippocampus and its subfields are not abundant. Thus, we aimed at understanding the changes and obtain a statistical model for the early prediction of Alzheimer's disease from the measures of hippocampal volume, hippocampal subfield volumes and the related covariates. We wanted to check if there were any differences in the predictive power of a statistical model based on the use of hippocampal volumes against that of hippocampal subfield volumes and the variations with respect to covariates. The wealth of information obtained from the imaging analysis must be statistically and computationally analyzed to obtain objective answers to the questions of interest.

3.2. Methods

Study participants

The regional ethics committee approved the research study and written consent were obtained from the participants (or family members or care givers where appropriate). The data presented in the current study are based on T1-weighted structural magnetic resonance images of 326 samples assembled by the National Research Center for Dementia (NRCD) at Chosun University in Gwangju, Republic of Korea. A battery of neuropsychological tests that assess language, attention, memory, visuospatial and executive function was administered to all participants. Controls samples did not show any evidence of neurological disease or impairment in cognitive function or activities of daily living. Alzheimer's disease samples were categorized based on the guidelines from the NINCDS-ADRDA for the clinical diagnosis of Alzheimer's disease (McKhann et al., 1984). Subjects with history of head trauma, focal lesion on brain MRI and medical or psychiatric causes that could affect cognitive decline were excluded.

MRI Acquisition

Contiguous 0.8 mm sagittal MPRAGE images of the whole brain examined at NRCD were acquired using 3T MR scanner (Skyra, Siemens) with the following parameters: TR = 2300 ms; TE = 2.143 ms; TI = 900 ms; 9 flip angle; FoV = 256x256; matrix = 320x320; number of slices = 178.

MRI preprocessing

High resolution structural T1-weighted images were processed using the FreeSurfer software package (Athinoula A. Martinos Center for Biomedical Imaging,

Harvard University, Cambridge, MA, USA) (v5.3.0) on a Linux environment using a 64-bit CentOS 7 operating system. The exclusive documentation of the freesurfer pipeline and methodologies can be found elsewhere (Dale et al., 1999, Fischl et al., 1999, Fischl et al., 2002, Fischl et al., 2004a, Fischl et al., 2004b). A complete automated processing including cortical and subcortical labelling using the Desikan-Killiany atlas was performed on each subject. The freesurfer processing stream involves performing motion correction, NU(non-uniform intensity normalization) for intensity inhomogeneity correction, image registration using affine transformation (6, 9 or 12 degrees of freedom) to Talairach space (J. Talairach, 1988) , and skull-stripping based on combination of watershed algorithm and deformable template model (Ségonne et al., 2004) or the removal of non-brain tissues. Then, the image volume is intensity normalized following non-linear warping of the atlas brain image to subject brain image which in turn is utilized in atlas-based tissue segmentation, in labeling the subcortical structures, brain stem, cerebellum, and cerebral cortex. The next step in FreeSurfer is to generate topologically correct cortical surface representation per hemisphere. Cortical surface lies either at the WM/GM tissue interface or at the GM/CSF tissue interface. Each hemisphere's cortical surface representation is mapped automatically to a standard spherical coordinate system. Key components of the surface mapping include surface inflation with minimal metric distortion, projection to spherical coordinates, topology correction, and surface based warping to align anatomically homologous points. Mapping to the standard spherical coordinate system

defined by FreeSurfer atlas brain allows for automated anatomical parcellation of cortex into gyral regions. Surface parcellation is then extended to GM volume, yielding parcellation of GM tissue sheet and regional cortical volumes. The entire computation took about 16-24 hours.

The hippocampal subfields were accessed using the Freesurfer v6.0.0, sub-dividing the hippocampus into subfields namely hippocampal tail(tail), subiculum(SUB), cornu ammonis 1(CA1), hippocampal fissure(fissure), presubiculum(PSUB), parasubiculum(ParaSUB), molecular layer(ML), granule cells/molecular layer/dentate gyrus (GCMLDG), cornu ammonis 3(CA3), cornu ammonis 4(CA4), fimbria, hippocampal-amygdala transition area(HATA) and the whole hippocampus (Iglesias et al., 2015).

Statistical analyses

All statistical analysis was performed using IBM SPSS Statistics (Version 23.0. Armonk, NY: IBM Corp.) One-way Analysis Of Variance (ANOVA) and Bonferroni post hoc correction for multiple comparisons was used for continuous demographic variables and Chi-squared test was performed on categorical demographic variables. The hippocampal subfield segmented volumes for left and the right hemispheres were individually calculated for all the participating subjects. The mean and standard deviation was calculated. Individual logistic regressions (Tibshirani, 1996) were fit using the hippocampal volumes (individual models with left-, right-, left-right and mean volumes) and hippocampal subfield volumes (individual models with left-, right-

, left-right and mean volumes). Analyses were performed separately for each hemispheres as evidences of asymmetries in the age associated brain changes are shown (Raz et al., 1997). Then, separate models with each covariates and different combinations of covariates were modelled. Accuracy, receiver operating characteristic (ROC) curve, sensitivity, specificity, positive predictive values and the negative predictive values were used as evaluation metrics

3.3. Results

The independent variable in the models with hippocampal volumes were the average volume of the whole hippocampus (volumes of left hemisphere, right hemisphere and mean of both hemispheres when mentioned) and in the models with the subfield volumes included the following variables: hippocampal tail (tail), subiculum (SUB), cornu ammonis 1(CA1), hippocampal fissure (fissure), presubiculum (PSUB), parasubiculum (ParaSUB), molecular layer (ML), granule cells/molecular layer/dentate gyrus (GCMLDG), cornu ammonis 3(CA3), cornu ammonis 4(CA4), fimbria and hippocampal-amygdala transition area (HATA) (volumes of left hemisphere, right hemisphere and mean of both hemispheres when mentioned).

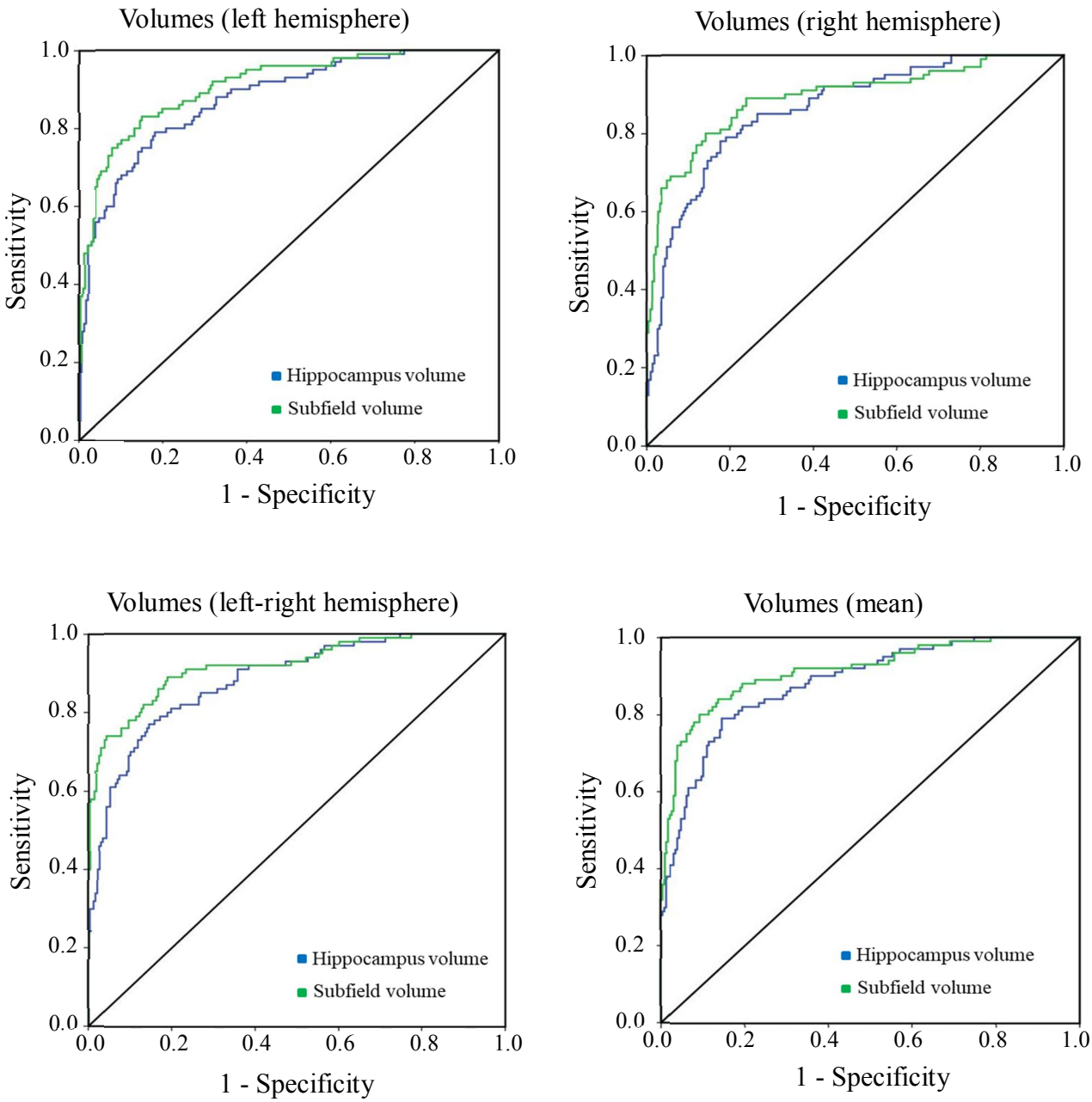

Figure 12, Receiver operator characteristic (ROC) curve for different models.

Metrics / Volumes	AUC	Sens	Spec	PPV	NPV
Left volumes					
Hippocampus	0.87	0.85	0.76	0.91	0.64
Subfield	0.90	0.87	0.81	0.92	0.71
Right volumes					
Hippocampus	0.86	0.83	0.75	0.91	0.59
Subfield	0.89	0.86	0.77	0.91	0.69
Left-Right volumes					
Hippocampus	0.88	0.86	0.75	0.90	0.67
Subfield	0.92	0.89	0.83	0.93	0.74
Mean volumes					
Hippocampus	0.88	0.85	0.74	0.90	0.64
Subfield	0.91	0.89	0.82	0.92	0.75

Table 7, Evaluation metrics for the ROC curve of different models. AUC; area under the curve, Sens; Sensitivity, Spec; Specificity, PPV; Positive predictive value, NPV; Negative predictive value.

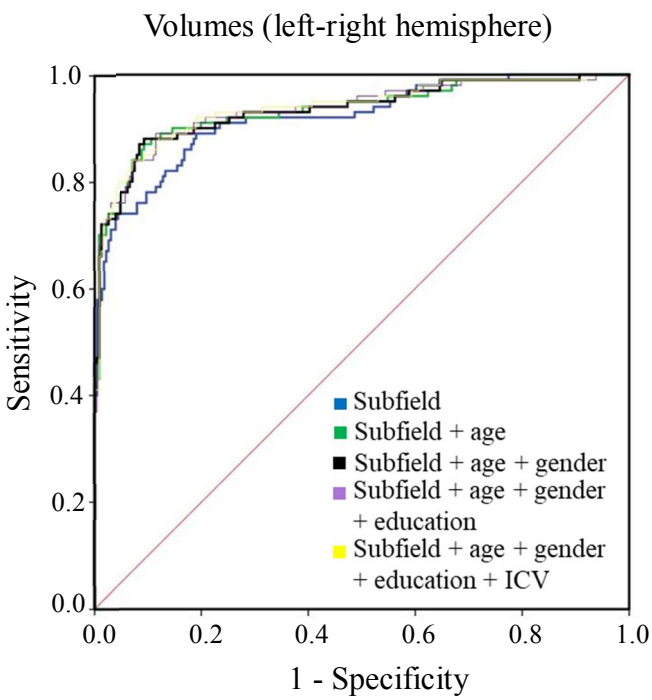

Figure 13, Receiver operator characteristic (ROC) curve for covariate models.

Metrics \ Models	Subfield	Subfield + age	Subfield + age + gender	Subfield + age + gender + education	Subfield + age + gender + education + ICV
AUC	0.92	0.93	0.93	0.93	0.93
Sens	0.89	0.90	0.90	0.90	0.91
Spec	0.83	0.86	0.87	0.85	0.86
PPV	0.93	0.94	0.95	0.94	0.94
NPV	0.74	0.78	0.78	0.78	0.80

Table 8, Evaluation metrics for the ROC curve of different covariate models. AUC; area under the curve, Sens; Sensitivity, Spec; Specificity, PPV; Positive predictive value, NPV; Negative predictive value.

3.4. Discussion

The current study investigated the performance of the statistical models using the hippocampal volumes, hippocampal subfield volumes and the influence in the predictive performance by the covariates for the early prediction of Alzheimer's disease. Though, the current study was a first step toward explaining the possibility of grouping individuals prior to detailed scrutiny for clinical trials. The present study to the best of our knowledge is the first in using the hippocampal subfields, sub-regions of one of the earliest regions affected in Alzheimer's disease for modeling.

Many studies have used the hippocampal volumes as the independent variable in their models for the prediction or classification of subjects into normal and abnormal (Sankar et al., 2017, Jack et al., 2013, Sabuncu et al., 2011). Though, it has been well-established that the hippocampus is heterogeneous structure, the subfield have not been used in the prediction models. In the present study, we investigated the predictive performance of the hippocampal volumes and the same with the hippocampal subfield volumes.

The predictive performance as evaluated by the area under the curve (AUC) and other metrics used showed that the hippocampal subfield volume provide us with greater number of features which enhance the power of the model used. One of the primary focuses of the current study was to check if the subfield volumes enhance the power of the prediction model. A very vital component of any prediction model is the predictive performance or the ability to classify subject's outcome and its clinical

relevance. Using the neuroanatomical regions, suggest the prospective trajectories of the prospective alterations in the brain structures and their repercussions. Subsequently, find out the initiation point of the prospective alterations in the brain structures.

To the best of our knowledge, this is the first study performed to understand the differences in predictive performance of hippocampal volumes and hippocampal subfield volume in classifying the normal and AD subjects. The findings from the study can be summarized as listed below:

Firstly, based on the results from the different models, the models obtained using the subfield volumes have always performed better than the models with the average hippocampal volumes. This reason maybe because the atrophy in the hippocampal subfields has been shown to be disproportional in multiple studies (Bobinski et al., 1998, Rössler et al., 2002, La Joie et al., 2013). However, while considering the entire hippocampal volumes, the gradual atrophy are not taken into account. The subfield models perform better than the hippocampal volume models as each subfield atrophies are captured clearly.

Secondly, while analyzing the results from the models with different covariates (with left-right subfield volumes), the addition or removal of a covariate did not prove to have high influence on the predictive performance of the model. Although, studies have shown age to have high influence on the normal and pathological aging, certain studies have shown that age and certain other covariates are not significant predictor of

hippocampal atrophy rate (Nosheny et al., 2015). Further, detailed studied would shed some light on the influence of the different covariate on the prediction model performances.

The study is a preliminary analysis with certain limitations such as no cross validations, use of simple models and small sample size.

Finally, models using other factors shown to influence AD can be used for to increase the prediction power. Application to multimodal imaging data would be promising future directions for biomarker discovery and better mechanistic understanding in AD research. Exploration of other imaging modalities as well as the combination of multiple modalities warrants further investigation with different independent variables and statistical models. Further effort may be made to include more complicated prior structure, like multiple layer groups or networks, to guide the learning procedure. Another possible future topic could be to investigate whether nonlinear models can help improve the prediction rates as well as derive biologically meaningful results.

Future studies aimed at age groups in the sixth decade or around the late fifties would help us in fitting a model that could better help in understanding the exact age around which the healthy cognitive aging would start to deviate from the path or change into pathological aging. Knowledge about the exact time of change will help in investigating the associated changes in the genetic, environmental, life style related

changes, dietary and nutritional changes, psychological and sexual dimorphic changes and changes in other possibly related factors.

References:

2018. 2018 Alzheimer's disease facts and figures. *Alzheimer's & Dementia,* 14**,** 367-429.

(UN), U. N. 2017. World Population Ageing.

ABE, O., YAMASUE, H., AOKI, S., SUGA, M., YAMADA, H., KASAI, K., MASUTANI, Y., KATO, N., KATO, N. & OHTOMO, K. 2008. Aging in the CNS: Comparison of gray/white matter volume and diffusion tensor data. *Neurobiology of Aging,* 29**,** 102-116.

ADASZEWSKI, S., DUKART, J., KHERIF, F., FRACKOWIAK, R. & DRAGANSKI, B. 2013. How early can we predict Alzheimer's disease using computational anatomy? *Neurobiol Aging,* 34**,** 2815-26.

AGUILAR, C., WESTMAN, E., MUEHLBOECK, J. S., MECOCCI, P., VELLAS, B., TSOLAKI, M., KLOSZEWSKA, I., SOININEN, H., LOVESTONE, S., SPENGER, C., SIMMONS, A. & WAHLUND, L. O. 2013. Different multivariate techniques for automated classification of MRI data in Alzheimer's disease and mild cognitive impairment. *Psychiatry Res,* 212**,** 89-98.

AIZENSTEIN, H., NEBES, R. D., SAXTON, J. A. & ET AL. 2008. Frequent amyloid deposition without significant cognitive impairment among the elderly. *Archives of Neurology,* 65**,** 1509-1517.

AKSU, Y., MILLER, D. J., KESIDIS, G., BIGLER, D. C. & YANG, Q. X. 2011. An MRI-derived definition of MCI-to-AD conversion for long-term, automatic prognosis of MCI patients. *PLoS One,* 6**,** e25074.

ALBERT, M. S., DEKOSKY, S. T., DICKSON, D., DUBOIS, B., FELDMAN, H. H., FOX, N. C., GAMST, A., HOLTZMAN, D. M., JAGUST, W. J., PETERSEN, R. C., SNYDER, P. J., CARRILLO, M. C., THIES, B. & PHELPS, C. H. 2011. The diagnosis of mild cognitive impairment due to Alzheimer's disease: Recommendations from the National Institute on Aging-Alzheimer's Association workgroups on diagnostic guidelines for Alzheimer's disease. *Alzheimer's & dementia : the journal of the Alzheimer's Association,* 7**,** 270-279.

ALLEN, J. S., BRUSS, J., BROWN, C. K. & DAMASIO, H. 2005. Normal neuroanatomical variation due to age: the major lobes and a parcellation of the temporal region. *Neurobiol Aging,* 26**,** 1245-60; discussion 1279-82.

ALLEN, J. S., DAMASIO, H. & GRABOWSKI, T. J. 2002. Normal neuroanatomical variation in the human brain: an MRI-volumetric study. *Am J Phys Anthropol,* 118**,** 341-58.

APOSTOLOVA, L. G., DUTTON, R. A., DINOV, I. D. & ET AL. 2006. Conversion of mild cognitive impairment to Alzheimer's disease predicted by hippocampal atrophy maps. *Archives of Neurology,* 63**,** 693-699.

ASHBURNER, J. & FRISTON, K. J. 2000. Voxel-based morphometry--the methods. *Neuroimage,* 11**,** 805-21.

BARTHEL, H., GERTZ, H. J., DRESEL, S., PETERS, O., BARTENSTEIN, P., BUERGER, K., HIEMEYER, F., WITTEMER-RUMP, S. M., SEIBYL, J., REININGER, C. & SABRI, O. 2011. Cerebral amyloid-beta PET with florbetaben (18F) in patients with Alzheimer's disease and healthy controls: a multicentre phase 2 diagnostic study. *Lancet Neurol,* 10**,** 424-35.

BATEMAN, R. J., XIONG, C., BENZINGER, T. L. S., FAGAN, A. M., GOATE, A., FOX, N. C., MARCUS, D. S., CAIRNS, N. J., XIE, X., BLAZEY, T. M., HOLTZMAN, D. M., SANTACRUZ, A., BUCKLES, V., OLIVER, A., MOULDER, K., AISEN, P. S., GHETTI, B., KLUNK, W. E., MCDADE, E., MARTINS, R. N., MASTERS, C. L., MAYEUX, R., RINGMAN, J. M., ROSSOR, M. N., SCHOFIELD, P. R., SPERLING, R. A., SALLOWAY, S. & MORRIS, J. C. 2012. Clinical and Biomarker Changes in Dominantly Inherited Alzheimer's Disease. *New England Journal of Medicine,* 367**,** 795-804.

BIGLER, E. D., ANDERSON, C. V. & BLATTER, D. D. 2002. Temporal lobe morphology in normal aging and traumatic brain injury. *AJNR Am J Neuroradiol,* 23**,** 255-66.

BOBINSKI, M., DE LEON, M. J., TARNAWSKI, M., WEGIEL, J., REISBERG, B., MILLER, D. C. & WISNIEWSKI, H. M. 1998. Neuronal and volume loss in CA1 of the hippocampal formation uniquely predicts duration and severity of Alzheimer's disease. *Brain Res,* 805**,** 267-9.

BOURGEAT, P., CHETELAT, G., VILLEMAGNE, V. L., FRIPP, J., RANIGA, P., PIKE, K., ACOSTA, O., SZOEKE, C., OURSELIN, S., AMES, D., ELLIS, K. A., MARTINS, R. N., MASTERS, C. L., ROWE, C. C. & SALVADO, O. 2010. Beta-amyloid burden in the temporal neocortex is related to hippocampal atrophy in elderly subjects without dementia. *Neurology,* 74**,** 121-7.

BRAAK, H. & BRAAK, E. 1991. Neuropathological stageing of Alzheimer-related changes. *Acta Neuropathologica,* 82**,** 239-259.

CARLESIMO, G. A., PIRAS, F., ORFEI, M. D., IORIO, M., CALTAGIRONE, C. & SPALLETTA, G. 2015. Atrophy of presubiculum and subiculum is the earliest hippocampal anatomical marker of Alzheimer's disease. *Alzheimer's & Dementia : Diagnosis, Assessment & Disease Monitoring,* 1**,** 24-32.

CEVENINI, E., CARUSO, C., CANDORE, G., CAPRI, M., NUZZO, D., DURO, G., RIZZO, C., COLONNA-ROMANO, G., LIO, D., DI CARLO, D., PALMAS, M. G., SCURTI, M., PINI, E., FRANCESCHI, C. & VASTO, S. 2010. Age-related inflammation: the contribution of different organs, tissues and systems. How to face it for therapeutic approaches. *Curr Pharm Des,* 16**,** 609-18.

CHOI, H. J., BYUN, M. S., YI, D., SOHN, B. K., LEE, J. H., LEE, J. Y., KIM, Y. K. & LEE, D. Y. 2017. Associations of thyroid hormone serum levels with in-vivo Alzheimer's disease pathologies. *Alzheimers Res Ther,* 9**,** 64.

CHOW, N., AARSLAND, D., HONARPISHEH, H., BEYER, M. K., SOMME, J. H., ELASHOFF, D., RONGVE, A., TYSNES, O. B., THOMPSON, P. M. & APOSTOLOVA, L. G. 2012. Comparing Hippocampal Atrophy in Alzheimer's Dementia and Dementia with Lewy Bodies. *Dementia and Geriatric Cognitive Disorders,* 34**,** 44-50.

COFFEY, C. E., LUCKE, J. F., SAXTON, J. A., RATCLIFF, G., UNITAS, L. J., BILLIG, B. & BRYAN, R. N. 1998. Sex differences in brain aging: a quantitative magnetic resonance imaging study. *Arch Neurol,* 55**,** 169-79.

CORDER, E. H., WOODBURY, M. A., VOLKMANN, I., MADSEN, D. K., BOGDANOVIC, N. & WINBLAD, B. 2000. Density profiles of Alzheimer's disease regional brain pathology for the Huddinge brain bank: pattern recognition emulates and expands upon Braak staging. *Experimental Gerontology,* 35**,** 851-864.

COSTAFREDA, S. G., DINOV, I. D., TU, Z., SHI, Y., LIU, C. Y., KLOSZEWSKA, I., MECOCCI, P., SOININEN, H., TSOLAKI, M., VELLAS, B., WAHLUND, L. O., SPENGER, C., TOGA, A. W., LOVESTONE, S. & SIMMONS, A. 2011. Automated hippocampal shape analysis predicts the onset of dementia in mild cognitive impairment. *Neuroimage,* 56**,** 212-9.

CUINGNET, R., GERARDIN, E., TESSIERAS, J., AUZIAS, G., LEHÉRICY, S., HABERT, M.-O., CHUPIN, M., BENALI, H. & COLLIOT, O. 2011. Automatic classification of patients with Alzheimer's disease from structural MRI: A comparison of ten methods using the ADNI database. *NeuroImage,* 56**,** 766-781.

DALE, A. M., FISCHL, B. & SERENO, M. I. 1999. Cortical Surface-Based Analysis: I. Segmentation and Surface Reconstruction. *NeuroImage,* 9**,** 179-194.

DECARLI, C., FRISONI, G. B., CLARK, C. M. & ET AL. 2007. Qualitative estimates of medial temporal atrophy as a predictor of progression from mild cognitive impairment to dementia. *Archives of Neurology,* 64**,** 108-115.

DELLI PIZZI, S., FRANCIOTTI, R., BUBBICO, G., THOMAS, A., ONOFRJ, M. & BONANNI, L. 2016. Atrophy of hippocampal subfields and adjacent extrahippocampal structures in dementia with Lewy bodies and Alzheimer's disease. *Neurobiology of Aging,* 40**,** 103-109.

DESIKAN, R. S., CABRAL, H. J., HESS, C. P., DILLON, W. P., GLASTONBURY, C. M., WEINER, M. W., SCHMANSKY, N. J., GREVE, D. N., SALAT, D. H., BUCKNER, R. L., FISCHL, B. & ALZHEIMER'S DISEASE NEUROIMAGING, I. 2009. Automated MRI measures identify individuals with mild cognitive impairment and Alzheimer's disease*. *Brain,* 132**,** 2048-2057.

DEVANAND, D. P., BANSAL, R., LIU, J., HAO, X., PRADHABAN, G. & PETERSON, B. S. 2012. MRI hippocampal and entorhinal cortex mapping in predicting conversion to Alzheimer's disease. *NeuroImage,* 60**,** 1622-1629.

DICKERSON, B. C., BAKKOUR, A., SALAT, D. H., FECZKO, E., PACHECO, J., GREVE, D. N., GRODSTEIN, F., WRIGHT, C. I., BLACKER, D., ROSAS, H. D., SPERLING, R. A., ATRI, A., GROWDON, J. H., HYMAN, B. T., MORRIS, J. C., FISCHL, B. & BUCKNER, R. L. 2009a. The cortical signature of Alzheimer's disease: regionally specific cortical thinning relates to symptom severity in very mild to mild AD dementia and is detectable in asymptomatic amyloid-positive individuals. *Cereb Cortex,* 19**,** 497-510.

DICKERSON, B. C., FECZKO, E., AUGUSTINACK, J. C., PACHECO, J., MORRIS, J. C., FISCHL, B. & BUCKNER, R. L. 2009b. Differential effects of aging and Alzheimer's disease on medial temporal lobe cortical thickness and surface area. *Neurobiol Aging,* 30**,** 432-40.

DORAISWAMY, P. M., SPERLING, R. A., JOHNSON, K., REIMAN, E. M., WONG, T. Z., SABBAGH, M. N., SADOWSKY, C. H., FLEISHER, A. S., CARPENTER, A., JOSHI, A. D., LU, M., GRUNDMAN, M., MINTUN, M. A., SKOVRONSKY, D. M., PONTECORVO, M. J. & GROUP, A. A. S. 2014. Florbetapir F 18 amyloid PET and 36-month cognitive decline:a prospective multicenter study. *Molecular Psychiatry,* 19**,** 1044.

DU, A.-T., SCHUFF, N., CHAO, L. L., KORNAK, J., JAGUST, W. J., KRAMER, J. H., REED, B. R., MILLER, B. L., NORMAN, D., CHUI, H. C. & WEINER, M. W. 2006. Age effects on atrophy rates of entorhinal cortex and hippocampus. *Neurobiology of aging,* 27**,** 733-740.

DU, A. T., SCHUFF, N., AMEND, D., LAAKSO, M. P., HSU, Y. Y., JAGUST, W. J., YAFFE, K., KRAMER, J. H., REED, B., NORMAN, D., CHUI, H. C. & WEINER, M. W. 2001. Magnetic resonance imaging of the entorhinal cortex and hippocampus in mild cognitive impairment and Alzheimer's disease. *J Neurol Neurosurg Psychiatry,* 71**,** 441-7.

DUVERNOY, H. M. 2005. *The human hippocampus : functional anatomy, vascularization, and serial sections with MRI,* Berlin; New York, Springer.

EWERS, M., WALSH, C., TROJANOWSKI, J. Q., SHAW, L. M., PETERSEN, R. C., JACK, C. R., JR., FELDMAN, H. H., BOKDE, A. L., ALEXANDER, G. E., SCHELTENS, P., VELLAS, B., DUBOIS, B., WEINER, M. & HAMPEL, H. 2012. Prediction of conversion from mild cognitive impairment to Alzheimer's disease dementia based upon biomarkers and neuropsychological test performance. *Neurobiol Aging,* 33**,** 1203-14.

FIRBANK, M. J., BLAMIRE, A. M., TEODORCZUK, A., TEPER, E., BURTON, E. J., MITRA, D. & O'BRIEN, J. T. 2010. High resolution imaging of the medial temporal lobe in Alzheimer's disease and dementia with Lewy bodies. *J Alzheimers Dis,* 21**,** 1129-40.

FISCHL, B., SALAT, D. H., BUSA, E., ALBERT, M., DIETERICH, M., HASELGROVE, C., VAN DER KOUWE, A., KILLIANY, R., KENNEDY, D., KLAVENESS, S., MONTILLO, A., MAKRIS, N., ROSEN, B. & DALE, A. M. 2002. Whole brain segmentation: automated labeling of neuroanatomical structures in the human brain. *Neuron,* 33**,** 341-55.

FISCHL, B., SALAT, D. H., VAN DER KOUWE, A. J. W., MAKRIS, N., SÉGONNE, F., QUINN, B. T. & DALE, A. M. 2004a. Sequence-independent segmentation of magnetic resonance images. *NeuroImage,* 23**,** S69-S84.

FISCHL, B., SERENO, M. I. & DALE, A. M. 1999. Cortical Surface-Based Analysis: II: Inflation, Flattening, and a Surface-Based Coordinate System. *NeuroImage,* 9**,** 195-207.

FISCHL, B., VAN DER KOUWE, A., DESTRIEUX, C., HALGREN, E., SEGONNE, F., SALAT, D. H., BUSA, E., SEIDMAN, L. J., GOLDSTEIN, J., KENNEDY, D., CAVINESS, V., MAKRIS, N., ROSEN, B. & DALE, A. M. 2004b. Automatically parcellating the human cerebral cortex. *Cereb Cortex,* 14**,** 11-22.

FJELL, A. M., MCEVOY, L., HOLLAND, D., DALE, A. M., WALHOVD, K. B. & ALZHEIMER'S DISEASE NEUROIMAGING, I. 2014a. What is normal in normal aging? Effects of aging, amyloid and Alzheimer's disease on the cerebral cortex and the hippocampus. *Progress in neurobiology,* 117**,** 20-40.

FJELL, A. M., WALHOVD, K. B., FENNEMA-NOTESTINE, C., MCEVOY, L. K., HAGLER, D. J., HOLLAND, D., BREWER, J. B. & DALE, A. M. 2009a. One-year brain atrophy evident in healthy aging. *J Neurosci,* 29**,** 15223-31.

FJELL, A. M., WESTLYE, L. T., AMLIEN, I., ESPESETH, T., REINVANG, I., RAZ, N., AGARTZ, I., SALAT, D. H., GREVE, D. N., FISCHL, B., DALE, A. M. & WALHOVD, K. B. 2009b. High consistency of regional cortical thinning in aging across multiple samples. *Cereb Cortex,* 19**,** 2001-12.

FJELL, A. M., WESTLYE, L. T., GRYDELAND, H., AMLIEN, I., ESPESETH, T., REINVANG, I., RAZ, N., DALE, A. M. & WALHOVD, K. B. 2014b. Accelerating cortical thinning: unique to dementia or universal in aging? *Cereb Cortex,* 24**,** 919-34.

FLEISHER, A., GRUNDMAN, M., JACK, C. R., JR & ET AL. 2005. Sex, apolipoprotein e ε4 status, and hippocampal volume in mild cognitive impairment. *Archives of Neurology,* 62**,** 953-957.

FLETCHER, E., VILLENEUVE, S., MAILLARD, P., HARVEY, D., REED, B., JAGUST, W. & DECARLI, C. 2016. β-amyloid, hippocampal atrophy and their relation to longitudinal brain change in cognitively normal individuals. *Neurobiology of aging,* 40**,** 173-180.

FOGWE, L. A. & MESFIN, F. B. 2018. Neuroanatomy, Hippocampus. *StatPearls.* Treasure Island (FL): StatPearls Publishing

StatPearls Publishing LLC.

FOX, N. C., CRUM, W. R., SCAHILL, R. I., STEVENS, J. M., JANSSEN, J. C. & ROSSOR, M. N. 2001. Imaging of onset and progression of Alzheimer's disease with voxel-compression mapping of serial magnetic resonance images. *Lancet,* 358**,** 201-5.

FRISONI, G. B., GANZOLA, R., CANU, E., RUB, U., PIZZINI, F. B., ALESSANDRINI, F., ZOCCATELLI, G., BELTRAMELLO, A., CALTAGIRONE, C. & THOMPSON, P. M. 2008. Mapping local hippocampal changes in Alzheimer's disease and normal ageing with MRI at 3 Tesla. *Brain,* 131**,** 3266-76.

GONZALEZ, C. E., PACHECO, J., BEASON-HELD, L. L. & RESNICK, S. M. 2015. Longitudinal changes in cortical thinning associated with hypertension. *J Hypertens,* 33**,** 1242-8.

GOOD, C. D., JOHNSRUDE, I. S., ASHBURNER, J., HENSON, R. N. A., FRISTON, K. J. & FRACKOWIAK, R. S. J. 2001. A Voxel-Based Morphometric Study of Ageing in 465 Normal Adult Human Brains. *NeuroImage,* 14**,** 21-36.

GORDON, B. A., BLAZEY, T., SU, Y. & ET AL. 2016. Longitudinal β-amyloid deposition and hippocampal volume in preclinical Alzheimer's disease and suspected non–Alzheimer's disease pathophysiology. *JAMA Neurology,* 73**,** 1192-1200.

GRIEVE, S. M., CLARK, C. R., WILLIAMS, L. M., PEDUTO, A. J. & GORDON, E. 2005. Preservation of limbic and paralimbic structures in aging. *Hum Brain Mapp,* 25**,** 391-401.

GRUNDMAN, M., SENCAKOVA, D., JACK, C. R., PETERSEN, R. C., KIM, H. T., SCHULTZ, A., WEINER, M. F., DECARLI, C., DEKOSKY, S. T., VAN DYCK, C., THOMAS, R. G. & THAL, L. J. 2002. Brain MRI hippocampal volume and prediction of clinical status in a mild cognitive impairment trial. *Journal of Molecular Neuroscience,* 19**,** 23-27.

HARADA, C. N., NATELSON LOVE, M. C. & TRIEBEL, K. 2013. Normal Cognitive Aging. *Clinics in geriatric medicine,* 29**,** 737-752.

HAVIGHURST, R. J. 1961. Successful Aging1. *The Gerontologist,* 1**,** 8-13.

HEBERT, L. E., WEUVE, J., SCHERR, P. A. & EVANS, D. A. 2013. Alzheimer's disease in the United States (2010–2050) estimated using the 2010 census. *Neurology,* 80**,** 1778.

HEDDEN, T., VAN DIJK, K. R., BECKER, J. A., MEHTA, A., SPERLING, R. A., JOHNSON, K. A. & BUCKNER, R. L. 2009. Disruption of functional connectivity in clinically normal older adults harboring amyloid burden. *J Neurosci,* 29**,** 12686-94.

HENNEMAN, W. J., SLUIMER, J. D., BARNES, J., VAN DER FLIER, W. M., SLUIMER, I. C., FOX, N. C., SCHELTENS, P., VRENKEN, H. & BARKHOF, F. 2009. Hippocampal atrophy rates in Alzheimer's disease: Added value over whole brain volume measures. *Neurology,* 72**,** 999-1007.

HINRICHS, C., SINGH, V., XU, G. & JOHNSON, S. 2009. MKL for robust multi-modality AD classification. *Med Image Comput Comput Assist Interv,* 12**,** 786-94.

HINRICHS, C., SINGH, V., XU, G. & JOHNSON, S. C. 2011. Predictive markers for AD in a multi-modality framework: an analysis of MCI progression in the ADNI population. *Neuroimage,* 55**,** 574-89.

HIPPIUS, H. & NEUNDÖRFER, G. 2003. The discovery of Alzheimer's disease. *Dialogues in clinical neuroscience,* 5**,** 101-108.

HORNAK, J. 2018. *Basics of NMR (Nuclear Magnetic Resonance)*.

HUTTON, C., DRAGANSKI, B., ASHBURNER, J. & WEISKOPF, N. 2009. A comparison between voxel-based cortical thickness and voxel-based morphometry in normal aging. *Neuroimage,* 48**,** 371-80.

IGLESIAS, J. E., AUGUSTINACK, J. C., NGUYEN, K., PLAYER, C. M., PLAYER, A., WRIGHT, M., ROY, N., FROSCH, M. P., MCKEE, A. C., WALD, L. L., FISCHL, B. & VAN LEEMPUT, K. 2015. A computational atlas of the hippocampal formation using ex vivo, ultra-high resolution MRI: Application to adaptive segmentation of in vivo MRI. *NeuroImage,* 115**,** 117-137.

J. TALAIRACH, P. T. 1988. *Co-Planar Stereotaxic Atlas of the Human Brain: 3-D Proportional System: An Approach to Cerebral Imaging,* New York, Thieme.

JACK, C. R., BARKHOF, F., BERNSTEIN, M. A., CANTILLON, M., COLE, P. E., DECARLI, C., DUBOIS, B., DUCHESNE, S., FOX, N. C., FRISONI, G. B., HAMPEL, H., HILL, D. L. G., JOHNSON, K., MANGIN, J.-F., SCHELTENS, P., SCHWARZ, A. J., SPERLING, R., SUHY, J., THOMPSON, P. M., WEINER, M. & FOSTER, N. L. 2011. Steps to standardization and validation of hippocampal volumetry as a biomarker in clinical trials and diagnostic criteria for Alzheimer's disease. *Alzheimer's & dementia : the journal of the Alzheimer's Association,* 7**,** 474-485.e4.

JACK, C. R., BENNETT, D. A., BLENNOW, K., CARRILLO, M. C., DUNN, B., HAEBERLEIN, S. B., HOLTZMAN, D. M., JAGUST, W., JESSEN, F., KARLAWISH, J., LIU, E., MOLINUEVO, J. L., MONTINE, T., PHELPS, C., RANKIN, K. P., ROWE, C. C., SCHELTENS, P., SIEMERS, E., SNYDER, H. M., SPERLING, R., ELLIOTT, C., MASLIAH, E., RYAN, L. & SILVERBERG, N. 2018. NIA-AA Research Framework: Toward a biological definition of Alzheimer's disease. *Alzheimer's & Dementia,* 14**,** 535-562.

JACK, C. R., JR., KNOPMAN, D. S., JAGUST, W. J., PETERSEN, R. C., WEINER, M. W., AISEN, P. S., SHAW, L. M., VEMURI, P., WISTE, H. J., WEIGAND, S. D., LESNICK, T. G., PANKRATZ, V. S., DONOHUE, M. C. & TROJANOWSKI, J. Q. 2013. Tracking pathophysiological processes in Alzheimer's disease: an updated hypothetical model of dynamic biomarkers. *Lancet Neurol,* 12**,** 207-16.

JACK, C. R., JR., PETERSEN, R. C., XU, Y., O'BRIEN, P. C., SMITH, G. E., IVNIK, R. J., TANGALOS, E. G. & KOKMEN, E. 1998. Rate of medial temporal lobe atrophy in typical aging and Alzheimer's disease. *Neurology,* 51**,** 993-999.

JACK, C. R., WISTE, H. J., KNOPMAN, D. S., VEMURI, P., MIELKE, M. M., WEIGAND, S. D., SENJEM, M. L., GUNTER, J. L., LOWE, V., GREGG, B. E., PANKRATZ, V. S. & PETERSEN, R. C. 2014. Rates of β-amyloid accumulation are independent of hippocampal neurodegeneration. *Neurology,* 82**,** 1605.

JACK, J. C. R., LOWE, V. J., WEIGAND, S. D., WISTE, H. J., SENJEM, M. L., KNOPMAN, D. S., SHIUNG, M. M., GUNTER, J. L., BOEVE, B. F., KEMP, B. J., WEINER, M., PETERSEN, R. C. & THE ALZHEIMER'S DISEASE NEUROIMAGING, I. 2009. Serial PIB and MRI in normal, mild cognitive impairment and Alzheimer's disease: implications for sequence of pathological events in Alzheimer's disease. *Brain,* 132**,** 1355-1365.

JAGUST, W. J., BANDY, D., CHEN, K., FOSTER, N. L., LANDAU, S. M., MATHIS, C. A., PRICE, J. C., REIMAN, E. M., SKOVRONSKY, D. & KOEPPE, R. A. 2010. The Alzheimer's Disease Neuroimaging Initiative positron emission tomography core. *Alzheimers Dement,* 6**,** 221-9.

JERNIGAN, T. L., ARCHIBALD, S. L., FENNEMA-NOTESTINE, C., GAMST, A. C., STOUT, J. C., BONNER, J. & HESSELINK, J. R. 2001. Effects of age on tissues and regions of the cerebrum and cerebellum. *Neurobiol Aging,* 22**,** 581-94.

JOHNSON, K. A., MINOSHIMA, S., BOHNEN, N. I., DONOHOE, K. J., FOSTER, N. L., HERSCOVITCH, P., KARLAWISH, J. H., ROWE, C. C., CARRILLO, M. C., HARTLEY, D. M., HEDRICK, S., PAPPAS, V. & THIES, W. H. 2013. Appropriate Use Criteria for Amyloid PET: A Report of the Amyloid Imaging Task Force, the Society of Nuclear Medicine and Molecular Imaging, and the Alzheimer's Association. *Journal of Nuclear Medicine,* 54**,** 476-490.

KALPOUZOS, G., CHETELAT, G., BARON, J. C., LANDEAU, B., MEVEL, K., GODEAU, C., BARRE, L., CONSTANS, J. M., VIADER, F., EUSTACHE, F. & DESGRANGES, B. 2009. Voxel-based mapping of brain gray matter volume and glucose metabolism profiles in normal aging. *Neurobiol Aging,* 30**,** 112-24.

KANASI, E., AYILAVARAPU, S. & JONES, J. 2016. The aging population: demographics and the biology of aging. *Periodontology 2000,* 72**,** 13-18.

KERCHNER, G. A., DEUTSCH, G. K., ZEINEH, M., DOUGHERTY, R. F., SARANATHAN, M. & RUTT, B. K. 2012. Hippocampal CA1 apical neuropil atrophy and memory performance in Alzheimer's disease. *NeuroImage,* 63**,** 194-202.

KILLIANY, R. J., HYMAN, B. T., GOMEZ-ISLA, T., MOSS, M. B., KIKINIS, R., JOLESZ, F., TANZI, R., JONES, K. & ALBERT, M. S. 2002. MRI measures of entorhinal cortex vs hippocampus in preclinical AD. *Neurology,* 58**,** 1188.

KLUNK, W. E., ENGLER, H., NORDBERG, A., WANG, Y., BLOMQVIST, G., HOLT, D. P., BERGSTROM, M., SAVITCHEVA, I., HUANG, G. F., ESTRADA, S., AUSEN, B., DEBNATH, M. L., BARLETTA, J., PRICE, J. C., SANDELL, J., LOPRESTI, B. J., WALL, A., KOIVISTO, P., ANTONI, G., MATHIS, C. A. & LANGSTROM, B. 2004. Imaging brain amyloid in Alzheimer's disease with Pittsburgh Compound-B. *Ann Neurol,* 55**,** 306-19.

KNOPMAN, D. S., JACK, C. R., LUNDT, E. S., WISTE, H. J., WEIGAND, S. D., VEMURI, P., LOWE, V. J., KANTARCI, K., GUNTER, J. L., SENJEM, M. L., MIELKE, M. M., MACHULDA, M. M., ROBERTS, R. O., BOEVE, B. F., JONES, D. T. & PETERSEN, R. C. 2015. Role of β-amyloidosis and Neurodegeneration in Subsequent Imaging Changes in Mild Cognitive Impairment. *JAMA neurology,* 72**,** 1475-1483.

KNOPMAN, D. S., JACK, C. R., WISTE, H. J., WEIGAND, S. D., VEMURI, P., LOWE, V. J., KANTARCI, K., GUNTER, J. L., SENJEM, M. L., MIELKE, M. M., ROBERTS, R. O., BOEVE, B. F. & PETERSEN, R. C. 2013. Selective Worsening of Brain Injury Biomarker

Abnormalities in Cognitively Normal Elderly with β-amyloidosis. *JAMA neurology,* 70**,** 10.1001/jamaneurol.2013.182.

KOHANNIM, O., HUA, X., HIBAR, D. P., LEE, S., CHOU, Y. Y., TOGA, A. W., JACK, C. R., JR., WEINER, M. W. & THOMPSON, P. M. 2010. Boosting power for clinical trials using classifiers based on multiple biomarkers. *Neurobiol Aging,* 31**,** 1429-42.

KOREA, S. 2017. Population Ageing. *2017 Statistics on the Aged.*

LA JOIE, R., PERROTIN, A., DE LA SAYETTE, V., EGRET, S., DOEUVRE, L., BELLIARD, S., EUSTACHE, F., DESGRANGES, B. & CHETELAT, G. 2013. Hippocampal subfield volumetry in mild cognitive impairment, Alzheimer's disease and semantic dementia. *Neuroimage Clin,* 3**,** 155-62.

LANDAU, S. M., HORNG, A., FERO, A., JAGUST, W. J. & FOR THE ALZHEIMER'S DISEASE NEUROIMAGING, I. 2016. Amyloid negativity in patients with clinically diagnosed Alzheimer's disease and MCI. *Neurology,* 86**,** 1377-1385.

LEMAITRE, H., CRIVELLO, F., GRASSIOT, B., ALPEROVITCH, A., TZOURIO, C. & MAZOYER, B. 2005. Age- and sex-related effects on the neuroanatomy of healthy elderly. *Neuroimage,* 26**,** 900-11.

LÓPEZ-OTÍN, C., BLASCO, M. A., PARTRIDGE, L., SERRANO, M. & KROEMER, G. 2013. The Hallmarks of Aging. *Cell,* 153**,** 1194-1217.

LUCASSEN, P., HEINE, V., MÜLLER, M., BEEK, E., M WIEGANT, V., DE KLOET, E., JOELS, M., FUCHS, E., SWAAB, D. & CZÉH, B. 2006. *Stress, Depression and Hippocampal Apoptosis*.

LUDERS, E., NARR, K. L., THOMPSON, P. M., REX, D. E., JANCKE, L. & TOGA, A. W. 2006a. Hemispheric asymmetries in cortical thickness. *Cereb Cortex,* 16**,** 1232-8.

LUDERS, E., NARR, K. L., THOMPSON, P. M., REX, D. E., WOODS, R. P., DELUCA, H., JANCKE, L. & TOGA, A. W. 2006b. Gender effects on cortical thickness and the influence of scaling. *Hum Brain Mapp,* 27**,** 314-24.

MAK, E., SU, L., WILLIAMS, G. B., WATSON, R., FIRBANK, M., BLAMIRE, A. & O'BRIEN, J. 2016. Differential Atrophy of Hippocampal Subfields: A Comparative Study of Dementia with Lewy Bodies and Alzheimer's disease. *Am J Geriatr Psychiatry,* 24**,** 136-43.

MCEVOY, L. K., HOLLAND, D., HAGLER, D. J., JR., FENNEMA-NOTESTINE, C., BREWER, J. B. & DALE, A. M. 2011. Mild cognitive impairment: baseline and longitudinal structural MR imaging measures improve predictive prognosis. *Radiology,* 259**,** 834-43.

MCKHANN, G., DRACHMAN, D., FOLSTEIN, M., KATZMAN, R., PRICE, D. & STADLAN, E. M. 1984. Clinical diagnosis of Alzheimer's disease: report of the NINCDS-ADRDA Work Group under the auspices of Department of Health and Human Services Task Force on Alzheimer's Disease. *Neurology,* 34**,** 939-44.

MCKHANN, G. M., KNOPMAN, D. S., CHERTKOW, H., HYMAN, B. T., JACK, C. R., KAWAS, C. H., KLUNK, W. E., KOROSHETZ, W. J., MANLY, J. J., MAYEUX, R., MOHS, R. C., MORRIS, J. C., ROSSOR, M. N., SCHELTENS, P., CARRILLO, M. C., THIES, B., WEINTRAUB, S. & PHELPS, C. H. 2011. The diagnosis of dementia due to Alzheimer's disease: Recommendations from the National Institute on Aging-Alzheimer's Association workgroups on diagnostic guidelines for Alzheimer's disease. *Alzheimer's & Dementia,* 7**,** 263-269.

MESULAM, M. M., WEINTRAUB, S., ROGALSKI, E. J., WIENEKE, C., GEULA, C. & BIGIO, E. H. 2014. Asymmetry and heterogeneity of Alzheimer's and frontotemporal pathology in primary progressive aphasia. *Brain,* 137**,** 1176-1192.

MINTUN, M. A., LAROSSA, G. N., SHELINE, Y. I., DENCE, C. S., LEE, S. Y., MACH, R. H., KLUNK, W. E., MATHIS, C. A., DEKOSKY, S. T. & MORRIS, J. C. 2006. [¹¹C]PIB in a nondemented population. *Neurology,* 67**,** 446.

MORMINO, E. C., BRANDEL, M. G., MADISON, C. M., RABINOVICI, G. D., MARKS, S., BAKER, S. L. & JAGUST, W. J. 2012. Not quite PIB-positive, not quite PIB-negative: slight PIB elevations in elderly normal control subjects are biologically relevant. *Neuroimage,* 59**,** 1152-60.

MORMINO, E. C., KLUTH, J. T., MADISON, C. M., RABINOVICI, G. D., BAKER, S. L., MILLER, B. L., KOEPPE, R. A., MATHIS, C. A., WEINER, M. W., JAGUST, W. J. & THE ALZHEIMER'S DISEASE NEUROIMAGING, I. 2009. Episodic memory loss is related to hippocampal-mediated β-amyloid deposition in elderly subjects. *Brain,* 132**,** 1310-1323.

MRAK, R. E., GRIFFIN, W. S. T. & GRAHAM, D. I. 1997. Aging-associated Changes in Human Brain. *Journal of Neuropathology & Experimental Neurology,* 56**,** 1269-1275.

MÜLLER, M. J., GREVERUS, D., DELLANI, P. R., WEIBRICH, C., WILLE, P. R., SCHEURICH, A., STOETER, P. & FELLGIEBEL, A. 2005. Functional implications of hippocampal volume and diffusivity in mild cognitive impairment. *NeuroImage,* 28**,** 1033-1042.

MURPHY, D. M., DECARLI, C., MCLNTOSH, A. R. & ET AL. 1996. Sex differences in human brain morphometry and metabolism: An in vivo quantitative magnetic resonance imaging and positron emission tomography study on the effect of aging. *Archives of General Psychiatry,* 53**,** 585-594.

NEWBERG, A. B. & ALAVI, A. 2010. *PET in the Aging Brain*, Saunders.

NEWGARD, C. B. & SHARPLESS, N. E. 2013. Coming of age: molecular drivers of aging and therapeutic opportunities. *The Journal of Clinical Investigation,* 123**,** 946-950.

NOSHENY, R. L., INSEL, P. S., TRURAN, D., SCHUFF, N., JACK, C. R., JR., AISEN, P. S., SHAW, L. M., TROJANOWSKI, J. Q., WEINER, M. W. & ALZHEIMER'S DISEASE NEUROIMAGING, I. 2015. Variables associated with hippocampal atrophy rate in normal aging and mild cognitive impairment. *Neurobiology of aging,* 36**,** 273-282.

OHNISHI, T., MATSUDA, H., TABIRA, T., ASADA, T. & UNO, M. 2001. Changes in brain morphology in Alzheimer's disease and normal aging: is Alzheimer's disease an exaggerated aging process? *AJNR Am J Neuroradiol,* 22**,** 1680-5.

ORGANIZATION, W. H. May 2017. *Dementia factsheet* [Online]. Available: http://www.who.int/mediacentre/factsheets/fs362/en/ [Accessed].

PIKE, K. E., SAVAGE, G., VILLEMAGNE, V. L., NG, S., MOSS, S. A., MARUFF, P., MATHIS, C. A., KLUNK, W. E., MASTERS, C. L. & ROWE, C. C. 2007. β-amyloid imaging and memory in non-demented individuals: evidence for preclinical Alzheimer's disease. *Brain,* 130**,** 2837-2844.

PRINCE, M., WIMO, A., GUERCHET, M., ALI, G., WU, Y. & PRINA, M. 2017. World Alzheimer Report 2015. The global impact of dementia. An analysis of prevalence, incidence, cost & trends. London: Alzheimer's Disease International; 2015. *World Health Organ-*

ization. Available from: https://www. alz. co. uk/research/World AlzheimerReport2015. pdf.[Cited April 15, 2016].

RAZ, N., GUNNING-DIXON, F. M., HEAD, D., DUPUIS, J. H. & ACKER, J. D. 1998. Neuroanatomical correlates of cognitive aging: evidence from structural magnetic resonance imaging. *Neuropsychology,* 12**,** 95-114.

RAZ, N., GUNNING, F. M., HEAD, D., DUPUIS, J. H., MCQUAIN, J., BRIGGS, S. D., LOKEN, W. J., THORNTON, A. E. & ACKER, J. D. 1997. Selective aging of the human cerebral cortex observed in vivo: differential vulnerability of the prefrontal gray matter. *Cerebral Cortex,* 7**,** 268-282.

REIMAN, E. M., CHEN, K., LIU, X., BANDY, D., YU, M., LEE, W., AYUTYANONT, N., KEPPLER, J., REEDER, S. A., LANGBAUM, J. B. S., ALEXANDER, G. E., KLUNK, W. E., MATHIS, C. A., PRICE, J. C., AIZENSTEIN, H. J., DEKOSKY, S. T. & CASELLI, R. J. 2009. Fibrillar amyloid-β burden in cognitively normal people at 3 levels of genetic risk for Alzheimer's disease. *Proceedings of the National Academy of Sciences,* 106**,** 6820.

ROBERTS, J. S., DUNN, L. B. & RABINOVICI, G. D. 2013. Amyloid imaging, risk disclosure and Alzheimer's disease: ethical and practical issues. *Neurodegenerative disease management,* 3**,** 219-229.

RODRIGUE, K. M. & RAZ, N. 2004. Shrinkage of the Entorhinal Cortex over Five Years Predicts Memory Performance in Healthy Adults. *The Journal of Neuroscience,* 24**,** 956.

RÖSSLER, M., ZARSKI, R., BOHL, J. & OHM, T. G. 2002. Stage-dependent and sector-specific neuronal loss in hippocampus during Alzheimer's disease. *Acta Neuropathologica,* 103**,** 363-369.

ROWE, C. C., ELLIS, K. A., RIMAJOVA, M., BOURGEAT, P., PIKE, K. E., JONES, G., FRIPP, J., TOCHON-DANGUY, H., MORANDEAU, L., O'KEEFE, G., PRICE, R., RANIGA, P., ROBINS, P., ACOSTA, O., LENZO, N., SZOEKE, C., SALVADO, O., HEAD, R., MARTINS, R., MASTERS, C. L., AMES, D. & VILLEMAGNE, V. L. 2010. Amyloid imaging results from the Australian Imaging, Biomarkers and Lifestyle (AIBL) study of aging. *Neurobiol Aging,* 31**,** 1275-83.

ROWE, J. W. & KAHN, R. L. 1987. Human aging: usual and successful. *Science,* 237**,** 143-9.

ROWE, J. W. & KAHN, R. L. 1997. Successful Aging1. *The Gerontologist,* 37**,** 433-440.

RUSINEK, H., DE SANTI, S., FRID, D., TSUI, W. H., TARSHISH, C. Y., CONVIT, A. & DE LEON, M. J. 2003. Regional brain atrophy rate predicts future cognitive decline: 6-year longitudinal MR imaging study of normal aging. *Radiology,* 229**,** 691-6.

SABUNCU, M. R., DESIKAN, R. S., SEPULCRE, J., YEO, B. T., LIU, H., SCHMANSKY, N. J., REUTER, M., WEINER, M. W., BUCKNER, R. L., SPERLING, R. A. & FISCHL, B. 2011. The dynamics of cortical and hippocampal atrophy in Alzheimer's disease. *Arch Neurol,* 68**,** 1040-8.

SALAT, D. H., BUCKNER, R. L., SNYDER, A. Z., GREVE, D. N., DESIKAN, R. S., BUSA, E., MORRIS, J. C., DALE, A. M. & FISCHL, B. 2004. Thinning of the cerebral cortex in aging. *Cereb Cortex,* 14**,** 721-30.

SANKAR, T., PARK, M. T. M., JAWA, T., PATEL, R., BHAGWAT, N., VOINESKOS, A. N., LOZANO, A. M. & CHAKRAVARTY, M. M. 2017. Your algorithm might think the hippocampus grows in Alzheimer's disease: Caveats of longitudinal automated hippocampal volumetry. *Hum Brain Mapp,* 38**,** 2875-2896.

SCHIPKE, C., PETERS, O., HEUSER, I., GRIMMER, T., SABBAGH, M. N., SABRI, O., HOCK, C., KUNZ, M., KUHLMANN, J., REININGER, C. & BLANKENBURG, M. 2012. *Impact of Beta-Amyloid-Specific Florbetaben PET Imaging on Confidence in Early Diagnosis of Alzheimer's Disease*.

SÉGONNE, F., DALE, A. M., BUSA, E., GLESSNER, M., SALAT, D., HAHN, H. K. & FISCHL, B. 2004. A hybrid approach to the skull stripping problem in MRI. *NeuroImage,* 22**,** 1060-1075.

SOLANA, R., TARAZONA, R., GAYOSO, I., LESUR, O., DUPUIS, G. & FULOP, T. 2012. Innate immunosenescence: effect of aging on cells and receptors of the innate immune system in humans. *Semin Immunol,* 24**,** 331-41.

SOWELL, E. R., PETERSON, B. S., THOMPSON, P. M., WELCOME, S. E., HENKENIUS, A. L. & TOGA, A. W. 2003. Mapping cortical change across the human life span. *Nat Neurosci,* 6**,** 309-15.

SPERLING, R. A., AISEN, P. S., BECKETT, L. A., BENNETT, D. A., CRAFT, S., FAGAN, A. M., IWATSUBO, T., JACK, C. R., KAYE, J., MONTINE, T. J., PARK, D. C., REIMAN, E. M., ROWE, C. C., SIEMERS, E., STERN, Y., YAFFE, K., CARRILLO, M. C., THIES, B., MORRISON-BOGORAD, M., WAGSTER, M. V. & PHELPS, C. H. 2011. Toward defining the preclinical stages of Alzheimer's disease: Recommendations from the National Institute on Aging-Alzheimer's Association workgroups on diagnostic guidelines for Alzheimer's disease. *Alzheimer's & Dementia,* 7**,** 280-292.

STORANDT, M., MINTUN, M. A., HEAD, D. & MORRIS, J. C. 2009. Cognitive decline and brain volume loss as signatures of cerebral amyloid-beta peptide deposition identified with Pittsburgh compound B: cognitive decline associated with Abeta deposition. *Arch Neurol,* 66**,** 1476-81.

TAUBE JEFFREY, S. 2004. Place cells recorded in the parasubiculum of freely moving rats. *Hippocampus,* 5**,** 569-583.

TERRY, R. D., DETERESA, R. & HANSEN, L. A. 1987. Neocortical cell counts in normal human adult aging. *Ann Neurol,* 21**,** 530-9.

TERRY, R. D., MASLIAH, E., SALMON, D. P., BUTTERS, N., DETERESA, R., HILL, R., HANSEN, L. A. & KATZMAN, R. 1991. Physical basis of cognitive alterations in Alzheimer's disease: synapse loss is the major correlate of cognitive impairment. *Ann Neurol,* 30**,** 572-80.

TIBSHIRANI, R. 1996. Regression Shrinkage and Selection via the Lasso. *Journal of the Royal Statistical Society. Series B (Methodological),* 58**,** 267-288.

TISSERAND, D. J. & JOLLES, J. 2003. On the Involvement of Prefrontal Networks in Cognitive Ageing. *Cortex,* 39**,** 1107-1128.

VAN DER GRAAF, M. 2010. In vivo magnetic resonance spectroscopy: basic methodology and clinical applications. *Eur Biophys J,* 39**,** 527-40.

VAN VELSEN, E. F., VERNOOIJ, M. W., VROOMAN, H. A., VAN DER LUGT, A., BRETELER, M. M., HOFMAN, A., NIESSEN, W. J. & IKRAM, M. A. 2013. Brain cortical thickness in the general elderly population: the Rotterdam Scan Study. *Neurosci Lett,* 550**,** 189-94.

VEMURI, P., GUNTER, J. L., SENJEM, M. L., WHITWELL, J. L., KANTARCI, K., KNOPMAN, D. S., BOEVE, B. F., PETERSEN, R. C. & JACK, C. R., JR. 2008. Alzheimer's disease diagnosis in individual subjects using structural MR images: validation studies. *Neuroimage,* 39**,** 1186-97.

VERHAEGHEN, P., MARCOEN, A. & GOOSSENS, L. 1993. Facts and Fiction About Memory Aging: A Quantitative Integration of Research Findings. *Journal of Gerontology,* 48**,** P157-P171.

VILLEMAGNE, V. L., BURNHAM, S., BOURGEAT, P., BROWN, B., ELLIS, K. A., SALVADO, O., SZOEKE, C., MACAULAY, S. L., MARTINS, R., MARUFF, P., AMES, D., ROWE, C. C. & MASTERS, C. L. 2013. Amyloid β deposition, neurodegeneration, and cognitive decline in sporadic Alzheimer's disease: a prospective cohort study. *The Lancet Neurology,* 12**,** 357-367.

VILLENEUVE, S., REED, B. R., MADISON, C. M., WIRTH, M., MARCHANT, N. L., KRIGER, S., MACK, W. J., SANOSSIAN, N., DECARLI, C., CHUI, H. C., WEINER, M. W. & JAGUST, W. J. 2014. Vascular risk and Aβ interact to reduce cortical thickness in AD vulnerable brain regions. *Neurology,* 83**,** 40-47.

WANG, L., MILLER, J. P., GADO, M. H., MCKEEL, D. W., ROTHERMICH, M., MILLER, M. I., MORRIS, J. C. & CSERNANSKY, J. G. 2006. Abnormalities of hippocampal surface structure in very mild dementia of the Alzheimer type. *NeuroImage,* 30**,** 52-60.

WEST, M. J., COLEMAN, P. D., FLOOD, D. G. & TRONCOSO, J. C. 1994. Differences in the pattern of hippocampal neuronal loss in normal ageing and Alzheimer's disease. *The Lancet,* 344**,** 769-772.

WEST, R. L. 1996. An application of prefrontal cortex function theory to cognitive aging. *Psychol Bull,* 120**,** 272-92.

WINKLER, A. M., KOCHUNOV, P., BLANGERO, J., ALMASY, L., ZILLES, K., FOX, P. T., DUGGIRALA, R. & GLAHN, D. C. 2010. Cortical thickness or grey matter volume? The importance of selecting the phenotype for imaging genetics studies. *NeuroImage,* 53**,** 1135-1146.

WORSLEY, K. J., E. TAYLOR, J., CARBONELL, F., CHUNG, M., DUERDEN, E., BERNHARDT, B., OC, L., BOUCHER, M. & EVANS, A. 2009. *SurfStat: A Matlab toolbox for the statistical analysis of univariate and multivariate surface and volumetric data using linear mixed effects models and random field theory*.

ZIEGLER, D. A., PIGUET, O., SALAT, D. H., PRINCE, K., CONNALLY, E. & CORKIN, S. 2010. Cognition in healthy aging is related to regional white matter integrity, but not cortical thickness. *Neurobiol Aging,* 31**,** 1912-26.

ACKNOWLEDGEMENT

I take this opportunity to thank my supervisor Prof. Kun Ho Lee, who has supported and contributed to the completion of my doctoral studies. I would also like to thank the rest of my thesis committee members, Prof. Jung Sup Lee, Prof. Byeong. C. Kim, Prof. Ho Yub Jong and Prof. Jungsoo Gim for all the valuable comments and suggestions.

I would like to extend my special thanks to all the lovely people in National Research Centre for Dementia for making it a great place. Foremost, I am greatly thankful to my neuroimaging mentor Prof. Yu Yong Choi for he had given me all the support, trainings, knowledge, time and the opportunity to work alongside. My statistics mentor Prof. Jang Jae Lee for all the technical training and being very cheerful and enthusiastic, every moment till the very end. Prof. Seok Cheol Lee for the friendly advises and support. Ms. Jeon Yeong Cho for the support in the lab. I would like to express my sincere gratitude to Prof. Kyu Yeong Choi, thank you very much for always willing to help and for all the care that you showered on me.

My graduation would have been virtually impossible without the complete support of my lab mates Mr. Tamil Iniyan Gunasekaran, Ms. Kang Sarang, Mr. Lim Hojae, Mr. Lee Dong Hee and Mr. Rhou Kyoung Min. Cheers and thanks to my other past lab mates and administrative staffs for the support throughout my PhD.

Finally, though it is beyond words, I express my sincere gratitude and appreciation to my entire family, extended family member and all the special people that I hold dear to my heart.